AD-A070 754 BIPHASE ENERGY SYSTEMS SANTA MONICA CA F/G 20/4

ANALYSIS OF TWO-PHASE FLOW IN NOZZLES AND TURBINE BUCKETS.(U)

JUN 79 E RITZI N00014-78-C-0649

UNCLASSIFIED 108-F NL

1 OF 2

AD
A070754

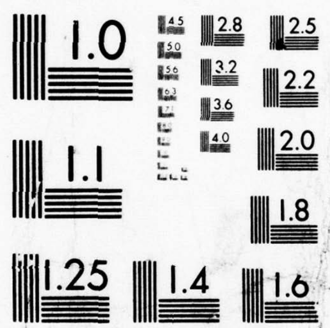

MICROCOPY RESOLUTION TEST CHART
NATIONAL BUREAU OF STANDARDS-1963-A

2800 Airport Avenue, Santa Monica, CA 90405
(213) 391-0691

LEVEL II

(12)

Biphase Energy Systems

Research-Cottrell

Report No. 108-F

FINAL REPORT

N-00014-78-C-0649

AD A070754

ANALYSIS OF TWO-PHASE FLOW IN NOZZLES AND TURBINE BUCKETS

by

Emil Ritzi
BIPHASE ENERGY SYSTEMS
Subsidiary of Research-Cottrell, Inc.
2800 Airport Avenue
Santa Monica, CA 90405

See 1473 in back

June 1, 1979

Final Report for Period
1 July 1978 to 30 April 1979

Prepared for

OFFICE OF NAVAL RESEARCH
DEPARTMENT OF THE NAVY
800 N. Quincy Street
Arlington, Virginia 22217

 The research was sponsored by the Office of Naval Research, Contract No. N-00014-78-C-0649 Work Unit 097-422.

ABSTRACT

The two-phase flow in a convergent-divergent nozzle was analyzed. The model used is that of one-dimensional equilibrium conditions, uniform temperature in a cross-section and zero wall friction. The liquid phase is assumed to consist of uniformly distributed spherical droplets of equal diameter, whose size is determined by the limiting Weber number breakup criterion. Smaller droplets may be fed to the nozzle initially. Formulas for mass-flux density, thrust and overall efficiency are given. The results provided by a computer program include the slip ratio (i.e. velocity ratio of the two phases) along the nozzle axis and the corresponding variation of the droplet size and the local friction losses due to droplet drag. The cone angle of the nozzle may be prescribed or it may be determined from a selected slip ratio gradient.

Initial conditions of slip ratio and droplet size required were investigated in detail. The ratio of droplet size to nozzle diameter is found to vary with nozzle size because of Reynolds and Weber number effects.

The slip model is found to predict a much higher mass-flux density at the throat than that given by the I.H.E. (Isentropic, Homogeneous, Equilibrium) model. Maximum mass-flux densities and minimum droplet sizes at the throat are outputs.

The two-dimensional two-phase flow in impulse turbine buckets was also investigated. The parameters that control the deviation angle of the droplets from the steam or gas path are identified.

ACKNOWLEDGMENT

Thanks are due especially to Karen Garcia and also Bill Baggenstoss for long, patient work with the computer program development. The report was edited by Dr. William Amend, and was produced by Hisa Olds with the help of Treva Meredith and Ying Chen. The bibliographical material was provided by Lance Hays who originated the idea for the study.

TABLE OF CONTENTS

LIST OF FIGURES

INTRODUCTION

Two-phase nozzles are employed to accelerate a cloud of liquid droplets suspended in a gaseous carrier to impart kinetic energy to the liquid phase for the purpose of driving a two-phase or liquid turbine. Large available pressure heads result in relatively modest discharge velocities of the mixtures because the droplets effectively increase the molecular weight of the mixture. Since the sonic velocity in the mixture is also lowered, the spouting velocity of the nozzle is generally supersonic, resulting in a converging-diverging geometry.

The performance of a two-phase nozzle is expected to increase with decreasing droplet size. A mathematical model has been developed to study the quantitative relationship between nozzle design, droplet size, and relative velocity or slip between the liquid and gaseous phases and the effects of irreversibilities. That is an important consideration, since the characteristics of the mixture will subsequently affect the turbine design and performance.

The simplest model would be the so-called Isentropic Homogeneous Equilibrium (IHE) model[1] which does not include slip and therefore friction losses or heat-transfer across the nozzle wall, nor does it admit any metastable states.[2,3]

The problems of supersonic nozzle design are the determination of the following:

1. Critical mass-flux density or the size of the throat area for a given mass flow rate.
2. The required area ratio (discharge area/throat area).
3. Predicted performance (efficiency) as a function of nozzle geometry, initial pressure, initial vapor fraction, approach velocity (and possibly time available for droplet breakup).

The first two may be well approximated for higher vapor fractions (i.e., $x > 0.2$) by the IHE model. However, the region of most interest in two-phase turbine applications is that for which the IHE model gives the poorest predictions. Thus a more sophisticated model that considers slip must be developed to enable nozzle predictions to be made for two-phase turbines.

The complexity of such an analysis depends on whether or not further evaporation occurs during the course of the expansion, which changes the vapor fraction.

Case I, with constant vapor fraction, is approached by two component systems consisting of a mixture of initially saturated or superheated steam and an oil of low vapor pressure.

Also, mixtures of air with water, initially at room temperature and elevated pressure, fall into that category.

Case II, with evaporation, is represented by single component systems exemplified by expanding wet steam.

Case III, which involves evaporation in a two-component system, is found for example in an initially pressurized, heated mixture of two liquids, to be expanded such that one liquid flashes into vapor. That case is not treated here in detail, since the emphasis was placed on Case II, the analysis of wet steam nozzle flow with droplets trailing the steam. The application of the analysis to Case I with constant vapor fraction which is realized for example in a mixture of water droplets in air is relatively easily made (it is a special, simpler case) but is not pursued further at this time.

Biphase Energy Systems presently has a computer code in its library that can predict nozzle performance in the region of interest. However, the code requires the input of a pressure profile along the nozzle axis, with the nozzle geometry being

an output. This restriction makes the off-design study of nozzle performance cumbersome. In particular, it is difficult to study the performance of straight conical nozzles (which are easy to make) with the present code. In addition, the existing program includes heat-transfer effects between the two phases which makes the analysis more cumbersome. Independent analysis and experimental results show that for small droplets the heat flux is very high and therefore a more simplified approach may concentrate on the more important influences on the droplet formation in a two-phase nozzle with slip.

Such a simplified analysis of the physical phenomena occurring in two-phase flow is presented in Part I.

While the progression of droplet breakup, of local friction losses between the slower moving droplets and the driving steam and the variation of the slip (or velocity) ratio is studied by means of the computer program which integrates numerically the differential equation for the slip ratio step by step along the expansion path, certain conclusions can be directly developed from the equations about the conditions at the nozzle inlet and at the throat. Some such results are the initial slip ratio and the ratio of droplet size to nozzle diameter at the inlet as a function of nozzle inlet size.

At the throat, upper limits of the mass-flux density can be determined as a function of temperature and slip ratio at the throat. Such results are of prime interest because of the considerable under-prediction of the mass-flow rate of wet steam nozzles with small initial vapor mass fractions by the simpler theories.

It will be seen that the theory given here indeed predicts higher mass-flux density, and also shows that small nozzles develop smaller droplets at the inlet, although somewhat larger than would be given by a direct proportion to the opening diameter. The initial slip ratio is correspondingly larger for the small nozzle. Lower inlet temperature and vapor fraction also make the achievement of good

nozzle performance a challenge. The study of the conditions at the nozzle inlet will determine the initial droplet size that needs to be fed to the nozzle in order to achieve certain performance objectives. The question of how the preatomization could most effectively be achieved is not treated here. A separate bibliography compiled in Appendix I gives an idea of the work already done in that area as well as other topics related to two-phase flow in turbines like erosion characteristics.

The results of Part I should primarily be considered as working tools for a design study of a two-phase engine. The formulations provided allow the calculation of all that is needed in a basic model study when the initial vapor fraction and the slip ratio are given. When these are unknown, they may be found by means of the computer program.

In Part II, two-phase flow in the turbine is considered. A result of the nozzle study is the final droplet size emerging from the nozzle. That leads to a consideration of whether more conventional turbines may be used effectively, that is without undue separation and impingement of droplets on the bucket walls. The formation of a thin liquid film on the buckets is associated with considerable friction losses because of the unfavorably small hydraulic diameter of such a film. Special bucket shapes that concentrate the film to a larger hydraulic diameter may alleviate the problem and were proposed in Reference 8. The deviation of the droplet path from the path of the gas is treated in Part II.

Besides the study of particle trajectories, a turbine design would have to be adapted to accommodate supersonic two-phase flow through the buckets at starting and design conditions. The reader is referred to items 8 to 13 in the Bibliography (page T-41, 42) of Reference 4.

The results of Part II may not enable final conclusions to be drawn concerning the general feasibility of two-phase impulse turbines. However, the tools given will form the basis for a specific study to be proposed.

APPROACH AND RESULTS

The present work uses first principles to develop the basic relationships that influence nozzle performance. The analysis is similar to that presented in References 5 and 6 which is very general when the loss mechanism is excluded. The loss formulation of References 5 and 6 used an impact (billiard ball) model between fluid elements moving at different velocities. The impact model is replaced in this work by the model employed by Elliott and Weinberg[7] which is based on the orderly movement of a cloud of spherical liquid droplets of equal diameter uniformly dispersed in the gaseous phase. Other assumptions used in the analysis are:

1. The fluids are in chemical and thermal equilibrium.

2. Flow is one-dimensional in the direction of the nozzle axis.

3. No friction at the wall.

4. Droplet breakup is controlled by a limiting Weber number criterion.

Since Reference 5 was based on the expansion of wet steam, the same single component fluid was used here, even though the consideration of Case II with continuously evaporating water droplets (and therefore changing vapor fraction) was more complicated analytically than the study of Case I with a constant vapor fraction. Also, the development of an algorithm for wet steam properties was considerably more involved than the use of ideal

gas properties. However, the potential practical usefulness of such a representation, particularly in a computer simulation, which includes viscosity and surface tension, was determined to justify the additional complexity.

The analysis is presented in detail in Part I. The first step was the formulation of the basic differential equation containing the derivative of the slip ratio with respect to pressure. A loss mechanism was not included in the early formulation, but, rather, the relative loss term $(1 - \eta_N)$ was employed as a parameter in the analysis. The simplified relationships (Equation (58) in Part I) were programmed on the computer and parameter sweeps were run to determine the initial slip ratio and droplet size without preatomization.

The next step was to formulate the relative loss based on the frictional drag of the trailing droplets. The initial slip ratio obtained from the simplified analysis was used to predict the relative loss of energy in the first increment of the nozzle. The resulting governing differential equation is given by Equation (90), which is an ordinary equation of the first order.

As pointed out in the introduction, a separate program was written for the determination of the initial slip ratio K to be used at the inlet to the nozzle. A criterion was found in the form of $dK/dp = 0$ (Equation (90)) which enables a limiting droplet size d_L to be determined for an assumed slip ratio K_L. Which d_L and K_L should then be used is a question of the droplet size that can be provided at the inlet. One approach is to use the Weber Number criterion for the droplet breakup which in effect gives another curve d_W as a function of K. The intersection of the d_W and d_L lines gives the solution at the nozzle inlet if no preatomization is provided for. Another approach is to prescribe the maximum droplet size at the nozzle inlet by the use of a separate preatomizer. The prescribed droplet diameter is then

set equal to d_L; the d_L curve pertaining to the selected inlet diameter will then give the initial slip ratio K.

The above study also provides a basis for a study of similarity relationships as, for example, the ratio of droplet to nozzle diameter at the nozzle inlet for geometrically similar nozzles. Reference 8 describes an investigation of similarity relations which was based upon small slip ratios. Conclusions were drawn as to the effect of vapor fraction and initial pressure levels. The loss formulation (Equation (82) and (83)) given in Part I shows that the ratio of droplet diameter to nozzle diameter is a significant non-dimensional parameter. It seems that a simple similarity rule were possible in terms of the initial droplet size/nozzle diameter ratio if it were not for the presence of the Reynolds number effect on the droplet drag coefficient. Also, use of the Weber number criterion for the droplet breakup introduces effects which cause deviations from a simple similarity rule based on an initial droplet size/nozzle diameter ratio. Details are given in Part I.

Besides the special study of the initial conditions required at the nozzle inlet, the general theory presented in Part I can also be used to establish limits of the mass-flux density at the nozzle throat. Conclusions regarding possible droplet size can also be drawn. Provided the slip ratio K is decreasing in the diverging part of the nozzle, the droplet size would be increasing according to the Weber number criterion. However, it is reasonable to assume that no coalescence of droplets occurs and that the droplet size reached at the throat will be maintained thereafter to the nozzle exit. That final droplet size will be important for the performance of a two-phase turbine.

As far as the workings of the computer program for the slip variation are concerned, no peculiarities or difficulties were encountered in the expansion of a two-phase mixture in the converging straight conical part of the nozzle. Much time, however,

was absorbed in interpreting the results for the diverging part of a nozzle. For small nozzles (with one centimeter inlet diameter) the slip ratio was large and the further expansion seemed to require a departure from the straight cone geometry. A trial and error adjustment of the cone angle was used to arrive at favorable conditions. See the end of Part I for further discussions.

On the whole it is felt that basic nozzle design tools were developed in the form of equations [for example Equations (21), (23), (26), (27), (30), (34), (37), (38), (57), (58), (79), (82) (83), (86) and (90)], and in the form of three computer programs: for the initial condition, for the limiting throat conditions and for the study of the entire expansion. An optimum nozzle design could not be concluded at this point, since no specific conditions or applications were defined as a requirement. More work is needed to define certain types of nozzle conditions and the corresponding design recommendations and performance potentials.

Since the nozzle performance study of Part I forms the basis for further two-phase turbine work (Part II), the latter could only be advanced to the development of basic procedures for its design work. Once the preatomization and nozzle expansion problem is sufficiently organized, more specific conclusions may be drawn for the turbine performance potentials in terms of the steam conditions, sizes and ratings. Since development work is in progress with liquid turbines a separate similar program for two-phase turbines should be initiated.

For a further discussion of results see "Conclusions and Recommendations".

PART I

ONE DIMENSIONAL MODEL FOR NOZZLE WITH SLIP

In the IHE model it was assumed that the velocity of the droplets, C_b , equals exactly the velocity of the gaseous carrier, C_a .

If we allow now a slip ratio

$$K \equiv C_a/C_b \geq 1.0$$

in a one-dimensional flow, (that is in a flow where uniform conditions prevail across any section at the length coordinate x^*), we must also distinguish between a volume or void fraction α of the gaseous phase (out of the total volume present at static conditions), and the vapor flow fraction, or quality, x which is the ratio of the gaseous mass flow rate, referred to the total mass flow per unit time at a given section.

While the mass density of the gaseous phase, referred to its volume is $1/v_a$, the mass density, referred to the total volume is α/v_a . The gaseous mass flux density, referred to the total cross-section is $\dot{m}_a/A = \alpha C_a/v_a$. By definition $\dot{m}_a/A = x\dot{m}_T/A$. Consequently, the total mass-flux density is

$$\dot{m}_T/A = \frac{\alpha C_a}{v_a x} \tag{1}$$

Considering that the static volume fraction of the liquid is $1-\alpha$ and its mass flow fraction $1-x$, the corresponding equation for the total mass-flux density is in terms of v_b is

$$\dot{m}_T/A = \frac{(1-\alpha)C_b}{v_b(1-x)} \tag{2}$$

Equating (1) and (2) allows α to be calculated when x , k and the density ratio v_b/v_a is known:

$$\frac{\alpha}{(1-\alpha)}K = \frac{x}{(1-x)}\frac{v_a}{v_b} \tag{3}$$

The static void fraction α corresponds only to the density corrected flow fraction x if the slip ratio K is unity; otherwise differences in velocity bring about changes in flow rates for the same void fractions. Equation (3) solved for $1/\alpha$ and $1/(1-\alpha)$ gives

$$\frac{1}{\alpha} = 1 + \frac{(1-x)}{x}\frac{v_b}{v_a}K \quad . \tag{4}$$

or

$$\frac{1}{1-\alpha} = 1 + \frac{x}{(1-x)}\frac{v_a}{v_b}\frac{1}{K} \tag{5}$$

The basic equations will now be formulated for the momentum, energy and continuity of the nozzle flow, following Reference 5. Neglecting frictional shear forces at the nozzle wall the momentum equation for steady flow is

$$Adp = -d(\dot{m}_a C_a + \dot{m}_b C_b) \tag{6}$$

$$= -d[\dot{m}_T(xC_a + (1-x)C_b)]$$

Since $\dot{m}_T$ is constant along the nozzle

$$dp = -\frac{\dot{m}_T}{A}\, d[xC_a + (1-x)C_b] \tag{7}$$

The velocities may be eliminated using Equations (1) and (2):

$$dp = -\left(\frac{\dot{m}_T}{A}\right) d\left[\left(\frac{\dot{m}_T}{A}\right)\left(\frac{x^2 v_a}{\alpha} + \frac{(1-x)^2 v_b}{(1-\alpha)}\right)\right] \tag{8}$$

Substitution of Equations (4) and (5) for α and $1-\alpha$ gives

$$dp = -\left(\frac{\dot{m}_T}{A}\right) d\left\{\left(\frac{\dot{m}_T}{A}\right)\left[x^2 v_a + x(1-x)\left[\frac{v_a}{K} + v_b K\right] + (1-x)^2 v_b\right]\right\} \quad (9)$$

Following Reference 5, the expression in brackets can be expressed as the product of the quantities $\bar{x}$ and $\bar{v}$ defined as follows:

$$\boxed{\bar{x} = x\sqrt{K} + \frac{(1-x)}{\sqrt{K}}} \quad (10)$$

and

$$\boxed{\bar{v} = \frac{x v_a}{\sqrt{K}} + (1-x) v_b \sqrt{K}\ .} \quad (11)$$

Using $\bar{x}$ and $\bar{v}$ Equation (9) becomes

$$\boxed{dp = -\left(\frac{\dot{m}_T}{A}\right) d\left\{\frac{\dot{m}_T}{A}\,\bar{x}\bar{v}\right\}} \quad (12)$$

The Energy Equation

With i_{m_o} defined as stagnation enthalpy of the mixture, we get

$$i_{m_o} = x\left(i_a + \frac{C_a^2}{2}\right) + (1-x)\left(i_b + \frac{C_b^2}{2}\right) \quad . \qquad (13)$$

The mixture enthalpy is

$$i_m = xi_a + (1-x)i_b \quad . \qquad (14)$$

Therefore

$$i_{m_o} = i_m + \frac{1}{2}\left[xC_a^2 + (1-x)C_b^2\right] \quad . \qquad (15)$$

The expression in the brackets may be defined as C_E^2. (See Equation (21) below.) Again eliminating C_a and C_b by means of Equations (1) and (2) we get

$$di_m = -\frac{1}{2}d\left\{\left(\frac{\dot{m}_T}{A}\right)^2\left[x^3\frac{v_a^2}{\alpha^2} + (1-x)^3\frac{v_b^2}{(1-\alpha)^2}\right]\right\} \qquad (16)$$

Using again Equations (4) and (5) we get

$$di_m = \frac{-1}{2}d\left\{\left(\frac{\dot{m}}{A}\right)^2\left[x^3v_a^2 + x^2(1-x)\left(2v_av_bK + \frac{v_a^2}{K^2}\right)\right.\right.$$
$$\left.\left. + x(1-x)^2\left(\frac{2v_av_b}{K} + v_b^2K^2\right) + (1-x)^3v_b^2\right]\right\} \quad . \qquad (17)$$

Using the definition (11) for $\bar{v}$ and the additional abbreviation

$$\boxed{\hat{x} = xK + \frac{1-x}{K}} \quad , \qquad (18)$$

it is seen that the expression in the square brackets of Equation (17) can be replaced by $\hat{x}\bar{v}^2$. The energy equation finally reads

$$\boxed{di_m = -\frac{1}{2} d \left\{ \left(\frac{\dot{m}_T}{A} \right)^2 \hat{x}\ \bar{v}^2 \right\}} \qquad (19)$$

Integrated between the stagnation point, where $\dot{m}_T/A = 0$ and a general point we get

$$\boxed{i_{m_o} - i_m = \frac{1}{2} \left(\frac{\dot{m}_T}{A} \right)^2 \hat{x}\ \bar{v}^2} \ . \qquad (20)$$

We are now in a position to formulate the deviations in velocity from the ideal slip and loss-free condition. When $K=1$, $\hat{x}=1$, $\bar{v}=v_m$ so that (20) yields

$$\boxed{i_{m_o} - i_m = \frac{1}{2} \left(\frac{\dot{m}_T v_m}{A} \right)^2 = \frac{C_E{}^2}{2}} \qquad (21)$$

which is the kinetic energy of the uniformly accelerated mixture. Note that C_E is not necessarily a result of an ideal isentropic expansion.

Combining Equations (1) and (4), the mass-flow density in terms of the gaseous velocity is

$$\boxed{\frac{\dot{m}_T}{A} = \frac{\alpha C_a}{v_a x} = \frac{C_a}{[x v_a + (1-x) v_b K]} = \frac{C_a}{\bar{v}\sqrt{K}}} \ . \qquad (22)$$

Equation (20) solved for $\dot{m}_T/A$, and with the definition (21) for C_E substituted gives

$$\boxed{\frac{\dot{m}_T}{A} = \left(\frac{1}{\sqrt{\hat{x}}\ \bar{v}}\right) C_E} \tag{23}$$

This equation expresses the mass-flux density in terms of the slip ratio K, the vapor mass fraction x, the specific volumes and the enthalpy change $C_E^2/2$.

Without slip the predicted mass-flow rate is

$$\left(\frac{\dot{m}_T}{A}\right)_{IHE} = \frac{C_S}{v_m} \tag{24}$$

The flow correction factor for the influence of slip therefore becomes

$$\frac{(\dot{m}_T)_K}{(\dot{m}_T)_{IHE}} = \left(\frac{v_m}{\bar{v}\sqrt{\hat{x}}}\right)^* \left(\frac{C_E}{C_S}\right)^* \tag{25}$$

The above factor may be applied to the formulas developed in a previous analysis for slip-free conditions. For a convergent-divergent nozzle the conditions at the throat are flow controlling; therefore the slip ratio K and the vapor mass fraction x have to be known at the throat.

Special values for the flow correction are as follows:

For $v_b << v_a$: $\quad \frac{v_m}{\bar{v}} \cong \sqrt{K}$

When x = 0: $\sqrt{\hat{x}} = \sqrt{\frac{1}{K}}$; $\frac{v_m}{\bar{v}\sqrt{\hat{x}}} \cong \sqrt{K}$.

When x = 1: $\sqrt{\hat{x}} = \sqrt{K}$; $\frac{v_m}{\bar{v}\sqrt{\hat{x}}} \cong 1.0$.

The result is that at low x values the presence of slip raises the flow over the no-slip prediction.

Equating Equations (22) and (23) yields

$$\boxed{C_a = \sqrt{\frac{K}{\hat{x}}}\, C_E} \tag{26}$$

Considering that $K \equiv C_a/C_b$ we also get

$$\boxed{C_b = \frac{1}{\sqrt{K\hat{x}}}\, C_E} \tag{27}$$

Note: Check of equations for special cases:

1) <u>x = 0</u> : $\hat{x} = \frac{1}{K}$; $C_a = KC_E$

$C_b = C_E$

When x = 0 there is no vapor; therefore intuitively:

$C_a = 0$ and $K = 0$, $\hat{x} \to \infty$.

2) <u>x = 1</u> : $\hat{x} = K$; $C_a = C_E$

$C_b = C_E/K$

When x = 1 there is no liquid; therefore $C_b = 0$, $K \to \infty$. The equations are found to work even under extreme conditions.

The significance of Equations (26) and (27) is that the phase velocities C_a and C_b are now expressed in terms of slip ratio K, vapor fraction x, and the energy velocity C_E that represents the enthalpy change of the mixture.

The thrust and nozzle efficiency may now be expressed similarly.

<u>Thrust</u>

Neglecting off-design conditions with possible deviations of the static pressure inside the nozzle from the back pressure, the axial thrust F is expressed as

$$F = \dot{m}_T [xC_a + (1-x)C_b]_{N2} \tag{28}$$

where the velocities C_a and C_b and the vapor mass fraction x are to be taken at the nozzle exit ("N2").

After substitution of Equations (26) and (27)

$$F = \dot{m}_T \left(\frac{C_E}{\sqrt{\hat{x}}}\right)_{N2} \left[x\sqrt{K} + (1-x)\frac{1}{\sqrt{K}}\right]_{N2} \tag{29}$$

The expression in brackets is recognized as $\bar{x}$ defined in Equation (10); therefore

$$\boxed{F = \dot{m}_T \left(C_E \frac{\bar{x}}{\sqrt{\hat{x}}}\right)_{N2}} \tag{30}$$

Again the result is expressed in terms of the slip ratio K at the nozzle exit and the vapor mass fraction x and the energy velocity

C_E at that station. The kinetic energy $C_E{}^2/2$ represents the enthalpy change of the mixture, which may differ from an isentropic change on account of friction losses inside the flow. The thrust correction factor on account of slip is (when $\dot{m}_T$ is considered a measured value)

$$\left(\frac{F_K}{F_{K=1}}\right) = \left(\frac{\bar{x}}{\sqrt{\hat{x}}}\right)_{N2} \tag{31}$$

where K and x are taken at the nozzle exit station. If the flow correction factor (27) is included, the thrust correction factor is

$$\boxed{\left(\frac{F_K}{F_{K=1}}\right)_{N2} = \left(\frac{\bar{x}}{\sqrt{\hat{x}}}\right)^{*}\left(\frac{\bar{x}}{\sqrt{\hat{x}}}\right)_{N2}} \tag{32}$$

Thrust Coefficient

We introduce the velocity $C_S = \sqrt{2(i_o - i_s)_m}$, which follows from an isentropic expansion from the stagnation condition i_{m_o}. The thrust coefficient may then be defined as

$$C_T = \frac{F}{\dot{m}_T C_S} = \frac{F}{\dot{m}_T C_E}\,\frac{C_E}{C_S} \tag{33}$$

Using Equation (30) we get

$$\boxed{C_T = \left(\frac{\bar{x}}{\sqrt{\hat{x}}}\right)_{N2}\left(\frac{C_E}{C_S}\right)} \tag{34}$$

Efficiency

An efficiency can be defined as

$$\eta_N = \frac{\dot{m}_a C_a^2/2 + \dot{m}_b C_b^2/2}{\dot{m}_T C_s^2/2}$$

$$= \frac{\left[x C_a{}^2 + (1-x) C_b{}^2\right]}{C_E{}^2} \left(\frac{C_E}{C_s}\right)^2 \qquad (35)$$

Substituting Equations (26) and (27) for C_a and C_b we get

$$\eta_N = \left[x \frac{K}{\hat{x}} + (1-x) \frac{1}{K\hat{x}}\right] \left(\frac{C_E}{C_s}\right)^2 \qquad (36)$$

Considering definition (18) for $\hat{x}$ reduces the expression in the brackets to unity (as it should be for the fulfillment of the energy Equation (15)). Therefore

$$\boxed{\eta_N = \left(\frac{C_E}{C_s}\right)^2} \qquad (37)$$

The slip losses show up only indirectly in the decrease of C_E below C_S due to friction losses on account of relative motion between the phases.

A "thrust efficiency" amounts to taking the square of the thrust coefficient, Equation (33):

$$\boxed{C_T{}^2 = \frac{(\bar{x})^2}{\hat{x}} \left(\frac{C_E}{C_s}\right)^2 = \frac{\bar{x}^2}{\hat{x}} \eta_N} \qquad (38)$$

In Reference 7 relative slips are defined. Correspondingly, the difference between C_a and C_b may be referred to the energy velocity C_E or to a momentum velocity C_M, where

$$\frac{C_E^2}{2} = x\frac{C_a^2}{2} + (1-x)\frac{C_b^2}{2} \tag{39}$$

$$C_M = \frac{F}{\dot{m}_T} = \left(C_E \frac{\bar{x}}{\sqrt{\hat{x}}} \right)_{N2} \tag{40}$$

Accordingly, from Equations (26) and (27)

$$S_E = \frac{C_a - C_b}{C_E} = \sqrt{\frac{K}{\hat{x}}} - \frac{1}{\sqrt{K\hat{x}}} = \frac{1}{\sqrt{\hat{x}}}\left(\sqrt{K} - \frac{1}{\sqrt{K}}\right) \tag{41}$$

$$S_M = \frac{C_a - C_b}{C_M} = \frac{\sqrt{\frac{K}{\hat{x}}} - \frac{1}{\sqrt{K\hat{x}}}}{\frac{\bar{x}}{\sqrt{\hat{x}}}} = \frac{1}{\bar{x}}\left(\sqrt{K} - \frac{1}{\sqrt{K}}\right) \tag{42}$$

The relative slip S depends therefore not only on K but also on the vapor mass fraction x.

Special cases:

$$x = 0; \quad \hat{x} = \frac{1}{K}, \quad \bar{x} = \frac{1}{\sqrt{K}}, \quad S_E = K-1 = S_M \tag{43}$$

$$x = 1; \quad \hat{x} = K, \quad \bar{x} = \sqrt{K}, \quad S_E = 1 - \frac{1}{K} = S_M \tag{44}$$

The Determination of the Slip Ratio K

The above relationships allow the calculation of mass-flow, thrust and efficiency when the slip ratio K, the vapor mass fraction x, and the specific volumes v_a and v_b are known at the throat and exit sections.

In a first part it will be shown that the combination of the momentum Equation (12) with the energy Equation (19) yields an ordinary differential equation of first order in K, provided the losses are known. This first part, which excludes the loss formulation, is independent of the form of the flow, that is, whether one or each of the phases form a connected space.

To this point the procedure will run parallel to that of Reference 5. A radical departure is then taken in the loss formulation from the impact model of Reference 5 to the frictional drag of a swarm of droplets, a procedure more similar to Reference 7.

The point of departure are equations (12) and (19)

$$dp = -\left(\frac{\dot{m}_T}{A}\right) d\left\{\frac{\dot{m}_T}{A}\,\bar{x}\,\bar{v}\right\} \qquad \text{(momentum)} \qquad (12)$$

$$di_m = -\frac{1}{2}\, d\left\{\left(\frac{\dot{m}_T}{A}\right)^2 \hat{x}\,\bar{v}^2\right\} \qquad \text{(energy)} \qquad (19)$$

Differentiation of the momentum Equation (12) gives

$$d\left(\frac{\dot{m}_T}{A}\cdot\bar{x}\,\bar{v}\right) = \frac{\dot{m}_T}{A}\, d(\bar{x}\,\bar{v}) + \bar{x}\,\bar{v}\, d\left(\frac{\dot{m}_T}{A}\right)$$

and

$$\boxed{-dp = \left(\frac{\dot{m}_T}{A}\right)^2 \left[d(\bar{x}\,\bar{v}) + \bar{x}\,\bar{v}\,\frac{d(\dot{m}_T/A)}{\dot{m}_T\, A}\right]} \qquad (45)$$

Similarly for Equation (19)

$$d\left\{\left(\frac{\dot{m}_T}{A}\right)^2 \hat{x}\ \bar{v}^2\right\} = \left(\frac{\dot{m}_T}{A}\right)^2 d(\hat{x}\ \bar{v}^2) + 2\,\hat{x}\,\bar{v}^2\left(\frac{\dot{m}_T}{A}\right) d\left(\frac{\dot{m}_T}{A}\right)$$

and

$$\boxed{-2di_m = \left(\frac{\dot{m}_T}{A}\right)^2 \hat{x}\ \bar{v}^2 \left\{\frac{d(\hat{x}\ \bar{v}^2)}{\hat{x}\ \bar{v}^2} + 2\,\frac{d(\dot{m}_T/A)}{\dot{m}_T/A}\right\}} \tag{46}$$

Substitution of Equation (13) for the mass-flux density and elimination of $\dfrac{d(\dot{m}_T/A)}{\dot{m}_T/A}$ between Equations (45) and (46) gives

$$di_m = \frac{\hat{x}}{\bar{x}}\,\bar{v}\ dp + \frac{C_E{}^2}{2}\left\{2\frac{d(\bar{x}\ \bar{v})}{\bar{x}\ \bar{v}} - \frac{d(\hat{x}\ \bar{v}^2)}{\hat{x}\ \bar{v}^2}\right\} \tag{47}$$

According to the laws of differentiation of products

$$\frac{d(\bar{x}\ \bar{v})}{\bar{x}\ \bar{v}} = \frac{d\bar{x}}{\bar{x}} + \frac{d\bar{v}}{\bar{v}} \tag{48}$$

$$\frac{d(\hat{x}\ \bar{v}^2)}{\hat{x}\ \bar{v}^2} = \frac{d\hat{x}}{\hat{x}} + 2\,\frac{d\bar{v}}{\bar{v}} \tag{49}$$

Substitution of (48) and (49) into (47) yields

$$di_m = \frac{\hat{x}}{\bar{x}}\,\bar{v}\ dp + \frac{C_E{}^2}{2}\left\{2\,\frac{d\bar{x}}{\bar{x}} - \frac{d\hat{x}}{\hat{x}}\right\} \tag{50}$$

Referring to the definitions (10) and (14) for $\bar{x}$ and $\hat{x}$, differentiation gives (when considering x and K as variables)

$$d\bar{x} = \frac{1}{2}\left[x\sqrt{K} - \frac{(1-x)}{\sqrt{K}}\right]\frac{dK}{K} + \left(\sqrt{K} - \frac{1}{\sqrt{K}}\right)dx \qquad (51)$$

$$d\hat{x} = \left[xK - \frac{(1-x)}{K}\right]\frac{dK}{K} + \left(K - \frac{1}{K}\right)dx \qquad (52)$$

The enthalpy change of the mixture, di_m may be eliminated by the definition of local efficiency, which is assumed to be known for the time being

$$\eta_N = \frac{di_m}{v_m dp} \qquad (53)$$

After substitution of (53) into (50) and multiplication of the equation by $\frac{\bar{x}\,\hat{x}}{C_E{}^2/2}$ we get

$$2\hat{x}(\hat{x}\,\bar{v} - \eta_N\,\bar{x}\,v_m)\frac{dp}{C_E{}^2} + 2\,\hat{x}d\bar{x} - \bar{x}d\hat{x} = 0 \qquad (54)$$

Substitution of Equations (51) and (52) into the last two terms of (54) after rearranging gives

$$2\,\hat{x}dx - \bar{x}d\hat{x} = \left(\sqrt{K} - \frac{1}{\sqrt{K}}\right)\left[(\hat{x} - 1)dx - 2x(1-x)\frac{dK}{K}\right] \qquad (55)$$

The first term of Equation (54) can be rearranged as follows

$$2\hat{x}(\hat{x}\,\bar{v} - \eta_N\,\bar{x}\,v_m)\frac{dp}{C_E{}^2} = \left[2\hat{x}(\hat{x}\,\bar{v} - \bar{x}\,v_m) + 2\,\hat{x}\,\bar{x}\,v_m(1 - \eta_N)\right]\frac{dp}{C_E{}^2}$$

$$= \left[-2x\hat{x}(1-x)\left(\sqrt{K} - \frac{1}{\sqrt{K}}\right)\left(\frac{v_a}{K} - Kv_b\right)\right.$$

$$\left. + 2\,\hat{x}\,\bar{x}\,v_m(1 - \eta_N)\right]\frac{dp}{C_E{}^2} \qquad (56)$$

Recombining Equations (55) and (56) yields

$$\boxed{\frac{dK}{K} - \frac{(\hat{x}-1)}{2x(1-x)}\,dx + \frac{dp}{C_E{}^2}\left\{\hat{x}\left(\frac{v_a}{K} - Kv_b\right) - \frac{\hat{x}\,\bar{x}\,v_m(1 - \eta_N)}{x(1-x)\left(\sqrt{K} - \frac{1}{\sqrt{K}}\right)}\right\} = 0} \qquad (57)$$

Multiplying by K/dp gives the alternate form

$$\frac{dK}{dp} - \frac{(\hat{x}-1)K}{2x(1-x)}\,\frac{dx}{dp} + \frac{K}{C_E{}^2}\left\{\frac{-\hat{x}\,\bar{x}\,v_m(1 - \eta_N)}{x(1-x)\left(\sqrt{K} - \frac{1}{\sqrt{K}}\right)} + \hat{x}\left(\frac{v_a}{K} - Kv_b\right)\right\} = 0 \qquad (58)$$

Equation (57) or (58) is the desired differential equation for K with p as the independent variable. The kinetic energy $C_E^2/2$ represents the enthalpy change from the stagnation condition to the pressure p at the inlet to the flow element investigated between two neighboring sections inside the nozzle. For <u>Case I</u>, with constant vapor fraction x, the second term for dx/dp becomes zero. In <u>Case II</u> with evaporation, for example, of wet steam dx/dp may be calculated according to Appendix II, which gives relationships for the calculation of steam properties.

Solutions of Equation (57) have been obtained for an assumed elemental relative loss $(1-\eta_N)$ for wet steam. It was found that certain limits in $(1-\eta_N)$ have to be observed.

Solution of Equation (57) turned out to be easier if $(1-\eta_N)$ is eliminated by a certain loss model to be treated next.

Loss Model

Consider a control volume of length dx^* and cross sectional area A containing n spherical droplets of diameter d. The ratio of liquid volume V_b to size of control volume V_c is

$$\frac{1}{\phi} = \frac{V_b}{V_c} = \frac{n\frac{\pi}{6}d^3}{Adx^*} \quad . \tag{59}$$

The liquid mass flow can then be expressed with the liquid velocity C_b and its specific volume v_b as follows

$$\dot{m}_b = \frac{C_b A}{v_b \phi} = \frac{C_b n\frac{\pi}{6}d^3}{v_b dx^*} \quad . \tag{60}$$

The total mass-flow follows

$$\dot{m}_t = \dot{m}_b/(1-x) \quad , \tag{61}$$

Assuming a drag force D_F between droplets and vapor defined by the drag coefficient C_D and the relative velocity $C_a - C_b$,

$$D_F = C_D \frac{1}{v_a} \frac{(C_a - C_b)^2}{2} \frac{\pi}{4} d^2 \quad . \tag{62}$$

The power loss of n droplets is, neglecting buoyancy

$$L = n\, D_F (C_a - C_b) \quad . \tag{63}$$

Here the droplets are considered spaced sufficiently far apart so that the flow around the spheres is not mutually influenced by neighboring spheres.

The loss per unit mass follows by dividing Equation (63) by Equation (61) with $\dot{m}_b$ according to Equation (60))

$$Tds = \frac{nD_F(C_a - C_b)\ v_b dx^*(1-x)}{n\ \frac{\pi}{6}\ d^3\ C_b} \qquad (64)$$

Substitution of D_F according to (62) gives

$$Tds = \frac{3}{2}\ C_D(1-x)\frac{v_b}{v_a}\ \frac{dx^*}{d}\ C_b{}^2(K-1)^3 \ . \qquad (65)$$

Eliminating C_b according to Equation (27), $C_b{}^2 = C_E{}^2/K\hat{x}$, yields

$$Tds = 3\ C_D\ \frac{(1-x)}{\hat{x}}\ \frac{v_b}{v_a}\ \frac{dx^*}{d}\ (K-1)^3\ \frac{C_E{}^2}{2K} \ . \qquad (66)$$

Considering that the relative loss is

$$1-\eta_N = \frac{-Tds}{v_m dp} \qquad (67)$$

we get

$$\boxed{1-\eta_N = -3\ C_D\ \frac{(1-x)}{\hat{x}}\ \frac{v_b}{v_a}\ \frac{dx^*}{dp}\ \frac{(K-1)^3}{K}\ \frac{C_E{}^2/2}{v_m d}} \ . \qquad (68)$$

Accordingly, the relative loss increases strongly with K ; the inverse dependency upon droplet size d is at first surprising. The contrary intuitive perception is that nozzle performance improves with smaller droplet size. It will be seen that indeed the final results confirm that expectation, after all terms are completely developed, especially the dependence of the slip ratio K on d. It was later found that Equation (68) is in agreement with Equation (78) and (79) of Reference 9.

Of all the quantities occurring in Equation (68), the length increment dx^* needs the most elaboration, since it needs to be expressed in terms of x , v_a , v_b , K , C_E , and dp .

Calculation of the Diameter Change dD and the Length Increment dx^*.

One possible way to express dx^* is via a mass-flux density change and therefore a diameter change. If the slope of the nozzle walls is assumed as known by the half angle δ, the diameter change dD is linked with dx^* according to

$$dD = 2dx^* \cdot \tan\delta \quad . \tag{69}$$

The sign convention for the half-angle δ can be selected such that for the converging part of the nozzle δ is taken as negative. That way dx^* will be positive throughout the nozzle.

The change in mass-flux density can be linked to the desired independent variables by means of the momentum equation. Combining Equations (45), (23) and (48) gives

$$\frac{-d(\dot{m}/A)}{\dot{m}/A} = \frac{\hat{x}\bar{v}}{\bar{x}}\frac{dp}{C_E{}^2} + \frac{d\bar{x}}{\bar{x}} + \frac{d\bar{v}}{\bar{v}} \tag{70}$$

Since the mass-flow rate is constant along the axis the left-hand side of Equation (44) can be reduced to

$$\frac{-d(\dot{m}/A)}{\dot{m}/A} = \frac{2dD}{D} \tag{71}$$

for a circular cross-section of diameter D.

Using Equation (71), the momentum Equation (70) becomes

$$2\frac{dD}{D} = \frac{\hat{x}\bar{v}}{x}\frac{dp}{C_E{}^2} + \frac{d\bar{x}}{\bar{x}} + \frac{d\bar{v}}{v} \tag{72}$$

where dD may be replaced by $2dx^* \tan\delta$.

Dividing the equation by dp gives

$$\boxed{S = \frac{2dx^*}{dp}\frac{\tan\delta}{D/2} = \frac{\hat{x}\bar{v}}{\bar{x}}\frac{1}{C_E{}^2} + \frac{d\bar{x}}{\bar{x}dp} + \frac{d\bar{v}}{\bar{v}dp} = \frac{2}{D}\frac{dD}{dp}} \tag{73}$$

for the momentum equation.

On the left hand side dx^*/dp constitutes the reciprocal of the axial pressure gradient.

In the case of <u>single phase flow</u> the change in mass-flux density is easily obtained as

$$d(\dot{m}/a) = d(\rho C) = \rho dC + Cd\rho \quad . \tag{74}$$

In normalized form, using the specific volume v instead of the density ρ we get

$$\frac{d(\dot{m}/A)}{(\dot{m}/A)} = \frac{dC}{C} - \frac{dv}{v} \quad . \tag{75}$$

Euler's equation for one-dimensional, gravity-free isentropic flow yields

$$\frac{dC}{C} = \frac{-vdp}{C^2} \quad . \tag{76}$$

Equations (75) and (76) combined give

$$\boxed{\frac{-d(\dot{m}/A)}{\dot{m}/A} = \frac{vdp}{C^2} + \frac{dv}{v}} \quad . \tag{77}$$

A comparison of the equation with Eq.(70) shows the meaning of the individual terms in Equation (70). $\hat{x}\bar{v}dp/\bar{x}C_E{}^2$ represents the effect of a relative velocity change; $d\bar{x}/\bar{x}$ constitutes the effect of a change in vapor fraction; $d\bar{v}/\bar{v}$ represents the influence of a specific volume change. For single phase flow, in the converging part of a nozzle the effect of the velocity increase more than offsets the increase in specific volume, therefore the mass-flux density progressively increases; in the diverging part the opposite is true. For two-phase flow the additional change in vapor fraction

appears and the effect of slip is present in the quantities $\hat{x}$, $\bar{x}$ and $\bar{v}$. To show the effect of changes in the slip ratio, dK, the differentials $d\bar{x}$ and $d\bar{v}$ have to be expressed in more basic terms.

On the right hand side of Equation (73) the differential $d\bar{x}$ was previously given in Equation (51). The differential $d\bar{v}$ is similarly derived from the definition of $\bar{v}$ in Equation (11) (when neglecting the change in the specific volume of the liquid)

$$\boxed{d\bar{v} = -\left[\frac{xv_a}{\sqrt{K}} - (1-x)\, v_b \sqrt{K}\right]\frac{dK}{2K} + \left(\frac{v_a}{\sqrt{K}} - v_b\sqrt{K}\right) dx + \frac{x}{\sqrt{K}}\, dv_a} \quad . \tag{78}$$

Substitution of $d\bar{x}$ and $d\bar{v}$ from Equations (51) and (78) gives for the momentum Equation (73)

$$\boxed{S = \frac{2}{D}\frac{dD}{dp} = \frac{2dx^*}{dp}\frac{\tan\delta}{D/2} = \frac{\hat{x}\bar{v}}{\bar{x}}\frac{1}{C_E{}^2} + \frac{V}{2K}\frac{dK}{dp} + Z\frac{dx}{dp} + \frac{x}{\bar{v}\sqrt{K}}\frac{dv_a}{dp}} \tag{79}$$

where V and Z are defined as follows

$$V = \frac{x\sqrt{K} - \dfrac{(1-x)}{\sqrt{K}}}{\bar{x}} - \frac{\left[\dfrac{xv_a}{\sqrt{K}} - (1-x)\, v_b\sqrt{K}\right]}{\bar{v}} \tag{80}$$

$$Z = \frac{\left(\sqrt{K} - \dfrac{1}{\sqrt{K}}\right)}{\bar{x}} + \frac{\left(\dfrac{v_a}{\sqrt{K}} - v_b\sqrt{K}\right)}{\bar{v}} \quad . \tag{81}$$

The derivative of the vapor specific volume dv_a/dp is given in the Appendix II.

Again, the right hand side of Equation (79) is a function of x, v_a, v_b, K, and C_E .

A discussion of the signs of each term will show whether its influence is increasing the mass-flux density (for positive terms) or the opposite. In the expansion of wet steam for example, the last term in Equation (79), $x\,dv_a/dp\ \bar{v}\sqrt{K}$ is always negative; Z is always positive, therefore Zdx/dp is always negative. The first term $\hat{x}\bar{v}/\bar{x}C_E{}^2$ is always positive. Since the first term in V is negative for small vapor fractions x , and since the second term of V approaches -1 in value, a flow with increasing slip $(dK/dp<o)$ will tend to give an increasing mass-flux density. If, in the overall effect, S is positive, the nozzle will be converging, with tanδ being negative.

The <u>relative loss</u>, Equation (47), may now be reformulated in terms of $S = 4dx^* \tan\delta/D\,dp$. For this purpose we define the following:

$$W = \frac{-3}{2} C_D \frac{(1-x)}{\hat{x}} \frac{v_b}{v_a} \frac{(K-1)^3}{K} \frac{D}{d\tan\delta} \quad . \qquad (82)$$

Equation (68) in terms of S and W now becomes

$$\boxed{1-\eta_N = \frac{WS\,C_E{}^2/4}{v_m}} \quad . \qquad (83)$$

Since W is dimensionless and S has the units of reciprocal pressure, the dimensions check.

The important conclusion is that the relative loss is not only determined by the slip ratio K and the droplet size d which are represented by W but the normalized inverse pressure gradient $SC_E{}^2/v_m$: good local efficiencies are possible with large K ratios.

Droplet Size

In order to evaluate W with Equation (82), the droplet size d must be known, so that the drag coefficient C_D can also be evaluated.

A criterion for the droplet size is that of a limiting Weber Number

$$We = \frac{(C_a - C_b)^2 d}{2v_a \sigma} \leq 6 \tag{84}$$

where σ is the surface tension, which is given in Appendix II. The droplet size limitations are given by

$$d \leq \frac{12\ v_a \sigma}{(C_a - C_b)^2} \ . \tag{85}$$

This criterion was used by Elliott in Reference 7; it also implies that the droplets are spherical in shape, and that they are all of the same diameter. A further discussion of the break-up criteria was already given for example by J.O. Hinze in 1947 in Reference 10.

Using the definition of the slip ratio K and Equation (27) for the liquid velocity C_b in terms of the energy velocity C_E of Equation (21), Equation (85) reduces to

$$\boxed{d \leq \frac{12\ v_a \sigma\ K\hat{x}}{C_E^2 (K-1)^2}} \ . \tag{86}$$

The drag coefficient C_D is a function of the Reynolds number, defined as

$$Re = \frac{d(C_a - C_b)}{v_a \eta_a} . \tag{87}$$

Reference 7 uses Stonecypher's least-square fit to Perry's tabulation as follows:

$$\begin{aligned} \ln C_D &= 3.271 - 0.8893 \ln Re \\ &+ 0.03417 (\ln Re)^2 \\ &+ 0.001443 (\ln Re)^3 , \end{aligned} \tag{88}$$

within the limits

$$0.1 < Re \leq 2 \times 10^4 .$$

Again, the Reynolds number may be expressed as a function of the basic variables

$$Re = \frac{d\, C_E\, (K-1)}{v_a \eta_a \sqrt{K \hat{x}}} . \tag{89}$$

In conclusion, W may now be calculated in terms of x, v_a, v_b, C_E, K, and the viscosity η_a (see Appendix II) by substituting Equations (86), (88), (89) into Equation (82).

The Final Differential Equation For The Slip Ratio K

We are now in a position to eliminate the unknown relative loss $1-\eta_N$ in Equation (58) by the use of the relation (83), where S has to be expressed by Equation (79). Fortunately the elimination of $1-\eta_N$ is possible without changing the character of the differential Equation (58) to find

$$\boxed{\frac{dK}{dp} = \frac{K\left\{\frac{\hat{x}-1}{2x(1-x)}\frac{dx}{dp} - \frac{\hat{x}}{C_E^2}\left(\frac{v_a}{K} - Kv_b\right) + \frac{W}{Q}\left[\frac{\hat{x}^2\bar{v}}{C_E^2} + \bar{x}\hat{x}R\right]\right\}}{1-\frac{\bar{x}\hat{x}WV}{2Q}}} \tag{90}$$

where

$$Q \equiv 4x(1-x)\left(\sqrt{K} - \frac{1}{\sqrt{K}}\right) \quad \text{and} \tag{91}$$

$$R \equiv Z\frac{dx}{dp} + \frac{x}{\bar{v}\sqrt{K}}\frac{dv_a}{dp} \quad . \tag{92}$$

Equation (90) also includes a term with dx/dp, the change of the vapor fraction with dp as the expansion progresses. The calculation of dx/dp for wet steam is given in the Appendix II.

With the conditions T, x, v_a, C_E, K, σ, η_a, dx/dp and the diameter D known <u>at the inlet</u> to a concical nozzle element, it is possible to calculate the droplet size d with Equation (86), the Reynolds number with Equation (89), the drag coefficient C_D with Equation (88), so that W follows from Equation (82). The derivative dK/dp follows then from Equation (90), and the relative diameter change $S = 2dD/D\,dp$ from Equation (79). A problem is posed by the <u>dependence on C_E</u> of dK/dp, of $d(\sim 1/C_E^2)$, of $Re\ (\sim C_E d)$ and of C_D, and therefore $W = f(C_E)$. The dependence on C_E is also present in S according to Equation (79), and in the local efficiency η_N.

While the enthalpy change, $C_E^2/2$, from the stagnation point to the inlet of the element that is being investigated may be assumed as known, the outlet value must be calculated for ready use in the next increment.

The static enthalpy change of the mixture, across the element considered, equals

$$di = \eta_N v_m dp \quad . \tag{93}$$

The local efficiency follows from the loss formula (83), whereas dp follows for wet steam from Clapeyron's equation, if dT is known

$$\frac{dp}{dT} = \frac{s_a - s_b}{v_a - v_b} = \frac{r_c}{T(v_a - v_b)} \quad , \tag{94}$$

where r_c is the heat of evaporation, given in the Appendix II.

The Influence of the Enthalpy Change $C_E^2/2$ Over a Nozzle Element

At first sight the elimination of $(1 - \eta_N)$ in Eq. (58) for dK/dp seems to make an iterative procedure unnecessary. However, since

$$C_E^2 = -2[(i - i_o) + \eta_N v_m dp] \quad , \tag{95}$$

and C_E is present in the formula for droplet size, for Re and therefore W, besides its direct presence in Eq. (90) for dK/dp, evaluation of dK/dp at successive points in the course of expansion over a nozzle element is affected by changes in dp within the element.

It is not possible to eliminate C_E and at the same time preserve the form of the differential Eq. (90) that is explicitly solved for dK/dp. The following iterative procedure was therefore followed.

The value of C_E^2 at the inlet to the nozzle element considered is assumed as known, either by being initially prescribed or by being carried over from the outlet of the previous element. As outlined before the values of d, Re, C_D and W may then be determined.

In order to eliminate the effect of C_E^2 on W, a new quantity W'' is defined

$$W'' = \frac{W}{4 v_m C_E^2} = \frac{-C_D (1-x)(K-1)^5 v_b D}{32\, \hat{x}^2 K^2 v_a^2 v_m \tan\delta\, \sigma} \tag{96}$$

which does not contain droplet size and C_E^2 directly. Similarly, the derivative S (Eq. (73)) can be expressed as

$$S = \left(R + \frac{V}{2K}\frac{dK}{dp}\right) + \frac{\hat{x}\bar{v}}{\bar{x} C_E^2} \tag{97}$$

The expression $(1 - \eta_N)/C_E^2$ in Eq.(58) for dK/dp can now be replaced by

$$\frac{1 - \eta_N}{C_E^2} = \frac{WS}{4v_m} = W''SC_E^2 \tag{98}$$

$$= W''\left[\left(R + \frac{V}{2K}\frac{dK}{dp}\right)C_E^2 + \frac{\hat{x}\bar{v}}{\bar{x}}\right]$$

After substitution into Eq.(58) we get

$$\boxed{\frac{dK}{dp} = \frac{\frac{(\hat{x}-1)K}{2x(1-x)}\frac{dx}{dp} - \frac{K}{C_E^2}\hat{x}\left(\frac{v_a}{K} - Kv_b\right) + A'W''\left(RC_E^2 + \frac{\hat{x}\bar{v}}{\bar{x}}\right)}{\left[1 - A'W''\frac{V}{2K}C_E^2\right]}} \tag{99}$$

where

$$A' = \frac{\hat{x}\,\bar{x}\,v_m K}{x(1-x)\left(\sqrt{K} - \frac{1}{\sqrt{K}}\right)} \quad . \tag{100}$$

The idea is to use the value of C_E^2 at the element entrance for a first approximation of dK/dp, according to Eq.(99), where C_E^2 occurs three times.

An improved value of C_E^2 is obtained as follows. From Eq. (98)

$$1 - \eta_N = W''\left(R + \frac{V}{2K}\frac{dK}{dp}\right)C_E^4 + W''\frac{\hat{x}\bar{v}}{\bar{x}}C_E^2 \quad .$$

Multiplying the above equation by $v_m dp$ (where dp is the pressure change from the inlet of the element to the particular station inside the element that is being considered) and eliminating η_N by

means of Eq.(93) yields a quadratic equation for C_E^2

$$\boxed{2W''\left(R + \frac{V}{2K}\frac{dK}{dp}\right)v_m dp C_E^4 + \left(2W''\frac{\hat{x}\bar{v}}{\tilde{x}}v_m dp - 1\right)C_E^2 - 2(\Delta i + v_m dp) = 0} \tag{101}$$

where $\Delta i = i_1 - i_o$, the enthalpy change from the stagnation conditions to the <u>inlet</u> of the element considered.

It was found that the minus sign in front of the square root of the discriminant gives the desired results for C_E^2. The result of Eq.(99) is used for dK/dp in Eq.(101). The new value of C_E^2 is then reintroduced into Eq.(99), where W'' is previously adjusted for the change in C_D. The recycling is stopped when initial and final values of C_E^2 agree within a certain relative error (10^{-6}).

Solving the Differential Equation

The differential Eq.(99) is an ordinary equation of the first order. Basically, at each temperature the properties v_a, v_b are known, and if the change in the vapor fraction dx/dT is predictable, as it is (see Appendix II), x is known and dv_a/dp, the change of specific volume of the vapor with respect to the pressure. If the derivative dK/dp were only a function of the pressure, a simple integration would do, but since the derivative dK/dp depends on the dependent variable, the slip ratio, K, a more elaborate procedure is required. (That dependence on K is present in the factor K itself, the compound quantities $\hat{x}$, $\bar{x}$, $\bar{v}$, Q, V, Z and R, which are all functions of t, x and K).

The Bulirsch-Stoer integration algorithm was selected, which is described in Ref. 11&12. The algorithm was extensively tested with varying step sizes in the nozzle program as well as in the solution of a test case in form of the differential equation $y' = -y$, which has as an exact solution the function $y = Ce^{-x}$. Assuming as given the function value $y = 1.0$ (C=1) at $x = 0$, together with the slope $y' = -1.0$, the Bulirsch-Stoer algorithm yielded the function value $y = 0.006738$ for the chosen step size of five $(x = 5)$. That agrees exactly within the six displayed digits with $y = e^{-5}$.

The algorithm consists of two parts, a discretization part and an extrapolation part. As the independent variable, (for example, temperature), is changed by a selected step size, approximate function values are determined in the first discretization part according to a procedure to be described next. Starting values are the function value and the derivative at the beginning of the step. Approximate function values are found at values of the independent variable that are found by subdividing into equal increments the total step, for example, by values N[H] = 1, 2, 3, 4, 6, 8, 12, 16, 24, 32 and 48, where H = 0, 1, 2, ..., 10. Figure 1

illustrates the procedure. Figure 1a shows the way a first approximation for the end point of the step is found. The same method is used for obtaining an approximate function value at the point nearest to the starting point of the step, as shown in Figure 1b. The same figure illustrates the procedure used to move on to the following point, C. The derivative or tangent is found at the preceding point, B, and a line is drawn parallel to the tangent, again through the preceding point A. The approximation to the function value at the end of the step is stored for each H = 0, 1, 2, ..., 48 into a matrix T[0,H] .

Second part: Extrapolation to zero step size. A rational function is used for that purpose. A two-dimensional matrix T[J,I] is constructed, with the integer I varying from zero to ten corresponding to the change in H from zero to ten. The columns are designated by the integers J. The approximate function values at the end of the step, T[0,H] form the column designated as J = 0. To the left of it (J = -1) a column of zeros is placed. The succeeding columns for J = 1, 2, ..., 9 are found recursively from the formula (Ref. 13).

$$T[J,I] = T[J-1,I+1] + \frac{T[J-1,I+1] - T[J-1,I]}{\left[\frac{h[I]}{h[I+J]}\right]^2 \left\{1 - \frac{T[J-1,I+1] - T[J-1,I]}{T[J-1,I+1] - T[J-2,I+1]}\right\} - 1} \qquad (102)$$

Such an extrapolation matrix is to be calculated for both the final value of the slip ratio K at the end of the step, and the final value of $C_E{}^2$, which is a measure of the enthalpy change to the end of the step. Typical values for the matrices are given in Table I. The last values, corresponding to T[J=9,I=1] and E[J=9,I=1] are finally used.

Note: Two special conditions have arisen when the convergence is very rapid: (a) The denominator T[J-1, I+1] - T[J-2, I+2] becomes zero; in that case the extrapolation may be terminated at that point; (b) The entire denominator [ ] { }-1 may become zero; in that case the very large default value for 1/0 of the computer was used for the quotient.

THE BULIRSCH-STOER DISCRETIZATION FOR N=1,2

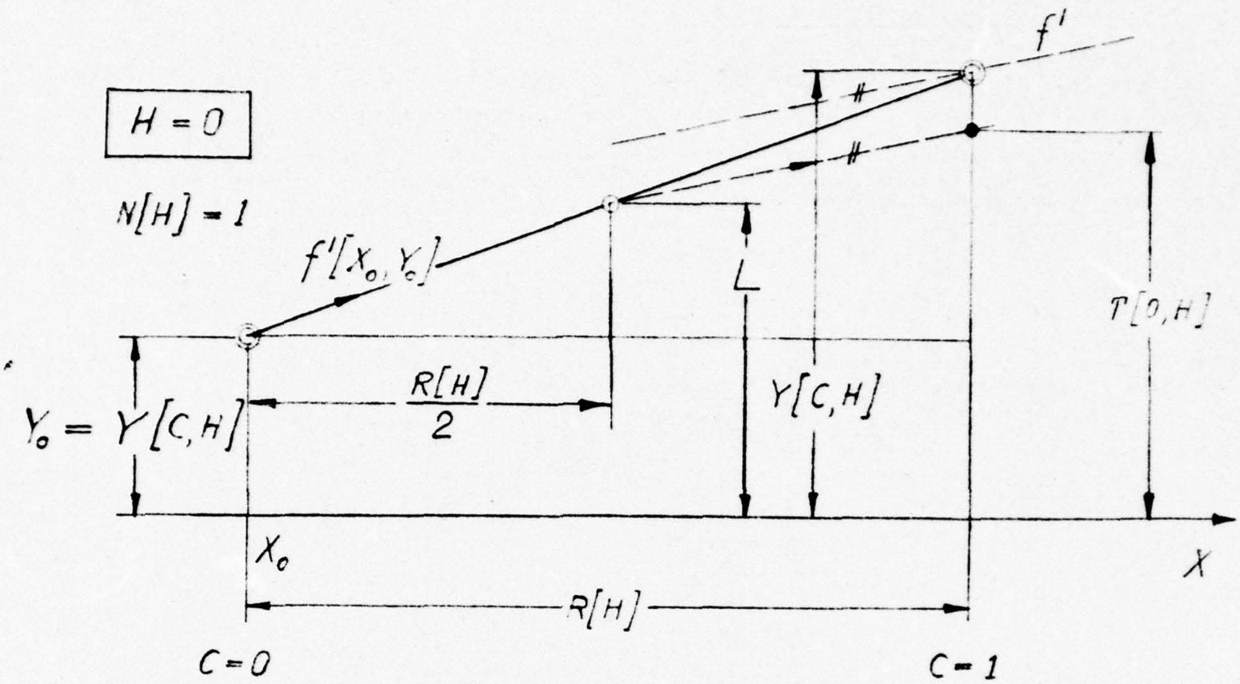

Figure 1a

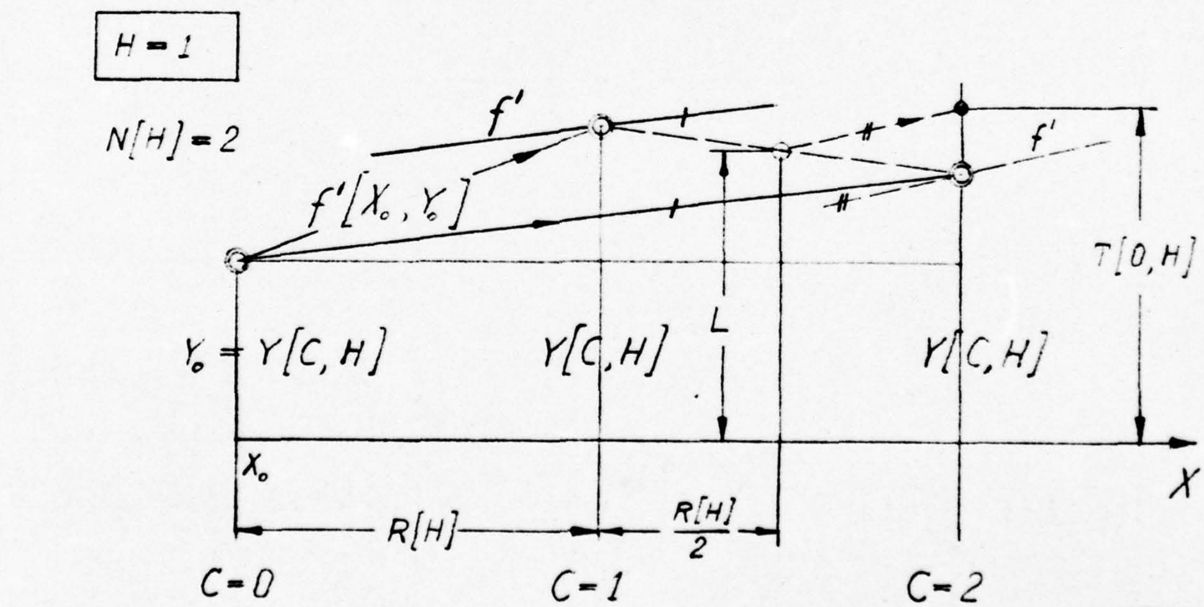

Figure 1b

Figure 1. Procedure for Solving the Differential Equation 4-23-79

Table 1. Solution Matrices for Slip Ratio and Enthalpy Change

T[J,I] MATRIX — STEP SIZE 0.25°C

I\J	0	1	2	3	4
0	2.693794	2.693661	2.693690	2.693685	2.693683
1	2.693694	2.693690	2.693676	2.693683	2.693682
2	2.693692	2.693686	2.693683	2.693681	2.693681
3	2.693689	2.693684	2.693681	2.693681	2.693679
4	2.693686	2.693682	2.693681	2.693680	2.693680
5	2.693685	2.693681	2.693680	2.693680	2.693676
6	2.693683	2.693681	2.693680	2.693679	2.693679
7	2.693682	2.693680	2.693679	2.693679	0.000000
8	2.693681	2.693680	2.693679	0.000000	0.000000
9	2.693680	2.693680	0.000000	0.000000	0.000000
10	2.693680	0.000000	0.000000	0.000000	0.000000

I\J	5	6	7	8	9
0	2.693680	2.693681	2.693680	2.693680	2.693678
1	2.693681	2.693680	2.693680	2.693680	$\boxed{2.693679} = K_2$
2	2.693681	2.693680	2.693679	2.693679	0.000000
3	2.693680	2.693680	2.693679	0.000000	0.000000
4	2.693680	2.693679	0.000000	0.000000	0.000000
5	2.693679	0.000000	0.000000	0.000000	0.000000
6	0.000000	0.000000	0.000000	0.000000	0.000000
7	0.000000	0.000000	0.000000	0.000000	0.000000
8	0.000000	0.000000	0.000000	0.000000	0.000000
9	0.000000	0.000000	0.000000	0.000000	0.000000
10	0.000000	0.000000	0.000000	0.000000	0.000000

E [J,I] MATRIX

I\J	0	1	2	3	4
0	2766.481628	2766.081376	2765.991353	2765.951776	2765.923368
1	2766.181429	2766.008628	2765.958896	2765.926913	2765.911481
2	2766.085426	2765.976526	2765.935236	2765.913948	2765.917195
3	2766.037781	2765.950025	2765.920021	2765.917097	2765.922832
4	2765.989027	2765.931152	2765.917496	2765.970505	2765.898256
5	2765.963706	2765.921882	2765.852380	2765.900079	2765.861309
6	2765.940470	2765.894940	2765.900810	2765.891655	2765.874392
7	2765.920550	2765.899610	2766.008755	2765.875619	0.000000
8	2765.908917	2765.857237	2765.877608	0.000000	0.000000
9	2765.886307	2765.875760	0.000000	0.000000	0.000000
10	2765.880448	0.000000	0.000000	0.000000	0.000000

I\J	5	6	7	8	9
0	2765.910613	2765.916724	2765.907135	2765.896062	2765.921942
1	2765.916993	2765.908338	2765.896255	2765.925809	$\boxed{2765.873004} = C_{E2}^2$
2	2765.911894	2765.896615	2765.939563	2765.873445	0.000000
3	2765.897175	2766.027232	2765.873896	0.000000	0.000000
4	2765.751926	2765.874370	0.000000	0.000000	0.000000
5	2765.874602	0.000000	0.000000	0.000000	0.000000
6	0.000000	0.000000	0.000000	0.000000	0.000000
7	0.000000	0.000000	0.000000	0.000000	0.000000
8	0.000000	0.000000	0.000000	0.000000	0.000000
9	0.000000	0.000000	0.000000	0.000000	0.000000
10	0.000000	0.000000	0.000000	0.000000	0.000000

The Stepping Procedure of the Program

For wet steam as a medium, temperature was selected as the independent variable. A step size is selected, an initial nozzle diameter, the initial slip ratio K is taken over from the result (final value) of the previous step (concerning the value at the inlet, see the next section) together with the vapor fraction x and the enthalpy change $(C_E^2/2)$ from the stagnation condition as reference. At the beginning of each step the mass-flux density $\dot{m}/A = C_E/(\bar{v}\sqrt{\hat{x}})$ is calculated. Since the mass-flux is the same along the nozzle axis, the ratio of the mass-flux densities from step to step equals the inverse of the cross-sectional area ratio, or

$$\frac{D_2}{D_1} = \sqrt{\frac{(\dot{m}/A)_1}{(\dot{m}/A)_2}} \quad . \tag{103}$$

A local efficiency can also be calculated, from the ratio of enthalpy change across a step to $v_m dp$:

$$\eta_N = \frac{\Delta C_E^2/2}{v_m dp} \quad . \tag{104}$$

The nozzle throat is defined by the maxiumum mass-flux density.

The Initial Condition

An initial kinetic energy can be prescribed together with an inlet diameter of the nozzle and the temperature and vapor fraction conditions. The initial slip ratio K can also be selected; however, experience with running the program suggests that K is best selected such as to make the derivative dK/dp at the inlet equal to zero, in order to avoid sharp adjustments in K at the beginning of the expansion in the nozzle.

When Eq. (90) for dK/dp is set equal to zero, a condition for a limiting value of W_L is obtained as follows

$$W_L = \frac{\left\{\frac{\hat{x}}{C_E{}^2}\left(\frac{v_a}{K} - Kv_b\right) - \frac{\hat{x} - 1}{2x(1-x)}\frac{dx}{dp}\right\} Q}{\left[\frac{\hat{x}^2\bar{v}}{C_E{}^2} + \bar{x}\,\hat{x}\,R\right]} \qquad (105)$$

where

$$Q = 4x(1-x)\left(\sqrt{K} - \frac{1}{\sqrt{K}}\right) \qquad (106)$$

$$R = Z\frac{dx}{dp} + \frac{x}{\bar{v}\sqrt{K}}\frac{dv_a}{dp} \qquad (107)$$

$$Z = \frac{\sqrt{K} - \frac{1}{\sqrt{K}}}{\bar{x}} + \frac{\frac{v_a}{\sqrt{K}} - v_b\sqrt{K}}{\bar{v}} \qquad (108)$$

The value W_L is a function of temperature (pressure), vapor fraction x, v_a and v_b, dx/dp, dv_a/dp, K and the initially assumed $C_E{}^2$. From the definition Eq. (82) for W follows

$$\frac{d_L}{C_D} = \frac{3}{2W_L \tan\delta}\frac{D}{v_a}\frac{v_b(1-x)}{\hat{x}}\frac{(K-1)^3}{K} \qquad (109)$$

In order to solve for the limiting droplet size, d_L, required to make $dK/dp = 0$, the expression for the Reynolds number (87) is divided by C_D as follows

$$\frac{Re}{C_D} = \frac{d_L C_E (K-1)}{C_D \sqrt{K\hat{x}} \; v_a \eta_a} \quad . \tag{110}$$

Eq. (109) for d_L/C_D may be substituted into the above Eq. (110) for Re/C_D. Since the drag coefficient C_D is a function of Re,

$$\ln C_D = A + By + Cy^2 + Dy^3 \tag{111}$$

where

$$y \equiv \ln Re \ , \tag{112}$$

C_D/Re may be expressed as a function of Re as follows

$$\ln\left(\frac{C_D}{Re}\right) = A + (B-1)y + Cy^2 + Dy^3 \ , \tag{113}$$

which leads to a cubic equation for y when C_D/Re is given

$$y^3 + \frac{C}{D} y^2 + \frac{B-1}{D} y + \frac{A + \ln(C_D/Re)}{D} = 0 \ . \tag{114}$$

Substitution of $y = x - \frac{C}{3D}$ leads to the cubic equation

$$x^3 + ax + b = 0 \tag{115}$$

where

$$a = \frac{B-1}{D} - \frac{1}{3}\left(\frac{C}{D}\right)^2 \tag{116}$$

$$b = \frac{A + \ln(C_D/Re)}{D} + \frac{2}{27}\left(\frac{C}{D}\right)^3 - \frac{1}{3}\frac{C}{D}\left(\frac{B-1}{D}\right) \ .$$

The discriminant follows

$$\Delta = \left(\frac{b}{2}\right)^2 + \left(\frac{a}{3}\right)^3 \tag{117}$$

If $\Delta < 0$, which is usually the case, there are three real solutions, including

$$x = 2\sqrt{-\frac{a}{3}}\cos(\phi + 240^{o}) \quad . \tag{118}$$

where ϕ follows from

$$\cos 3\phi = \frac{-b}{2\sqrt{\left(-\frac{a}{3}\right)^3}} \quad . \tag{119}$$

The values of the constants are, according to Eq. (88) A = 3.271, B = -0.8893, C = 0.03417, D = 0.001443, so that a = -1496.198 and $(a/3)^3 = -1.240518 \times 10^8$. The constant b/2 becomes

$$b/2 = 6792.464 + 346.5 \ln(Re/C_D) \tag{120}$$

and y = x - 7.89328.

As the slip ratio K is varied, the limiting d_L required to make $dK/dp = 0$ may be calculated. A typical plot is shown in Figure 2. The relative loss $(1 - \eta_N)$ encountered due to the dragging of the droplets may be calculated and plotted on the same figure. At the same time the Weber Number criterion yields a droplet size d_W from Eq. (86), which may also be plotted as a function of K. It is seen in Figure 2 that the d_L and d_W lines intersect at some K value. That value of the slip ratio is the one to be used initially if no pre-atomization is provided before the nozzle and the "Weber breakup" is assumed. It was found that indeed when such an initial K value was used with the main program the slip would initially obey $dK/dp = 0$.

Similarity - The initial value problem for K just described gives the possibility of studying the performance of geometrically similar

nozzles of a certain ratio of droplet size to nozzle diameter at the inlet. Figures 2, 3, 4 and 5 show the "limiting droplet size d_L" required to give $dK/dp = 0$ for different size nozzles (D = 0.005, 0.01, 0.1 and 0.2 m). While the magnitude of W_L is independent of nozzle diameter, d_L/C_D contains D in Eq. (109). The loss curve $(1 - \eta_N)$, however, is independent of diameter since S of Eq. (79) is independent of D and

$$1 - \eta_N = \frac{W_L \; S \; C_E^2}{4 \, v_m} \; .$$

Similarly, the droplet size according to the Weber criterion is independent of nozzle diameter D, according to Eq. (86)

$$d_W \leqq \frac{12 \; v_a \sigma K \; \hat{x}}{C_E^2 (K - 1)^2} = f(t, x, K, C_E^2) \; . \quad (121)$$

The points of intersection of the lines d_L and d_W move to smaller K ratios as the nozzle size increases. The droplet size, following the d_W curve increases correspondingly. The ratio D/d_L varies with K and D as follows:

D	K_o	$d_L = d_W$	D/d	$1-\eta_N$	η_N
m	-	μm	-	-	-
0.01	4.30	190	52.63	0.478	0.522
0.025	3.50	255	98.04	0.488	0.512
0.05	3.04	335	149.25	0.430	0.570
0.1	2.68	435	229.88	0.462	0.538
0.2	2.39	578	346.02	0.442	0.558
0.5	2.09	855	584.80	0.410	0.590
for $dK/dp = 0$					

The result is that the ratio of the nozzle and droplet diameters decreases for smaller nozzles.

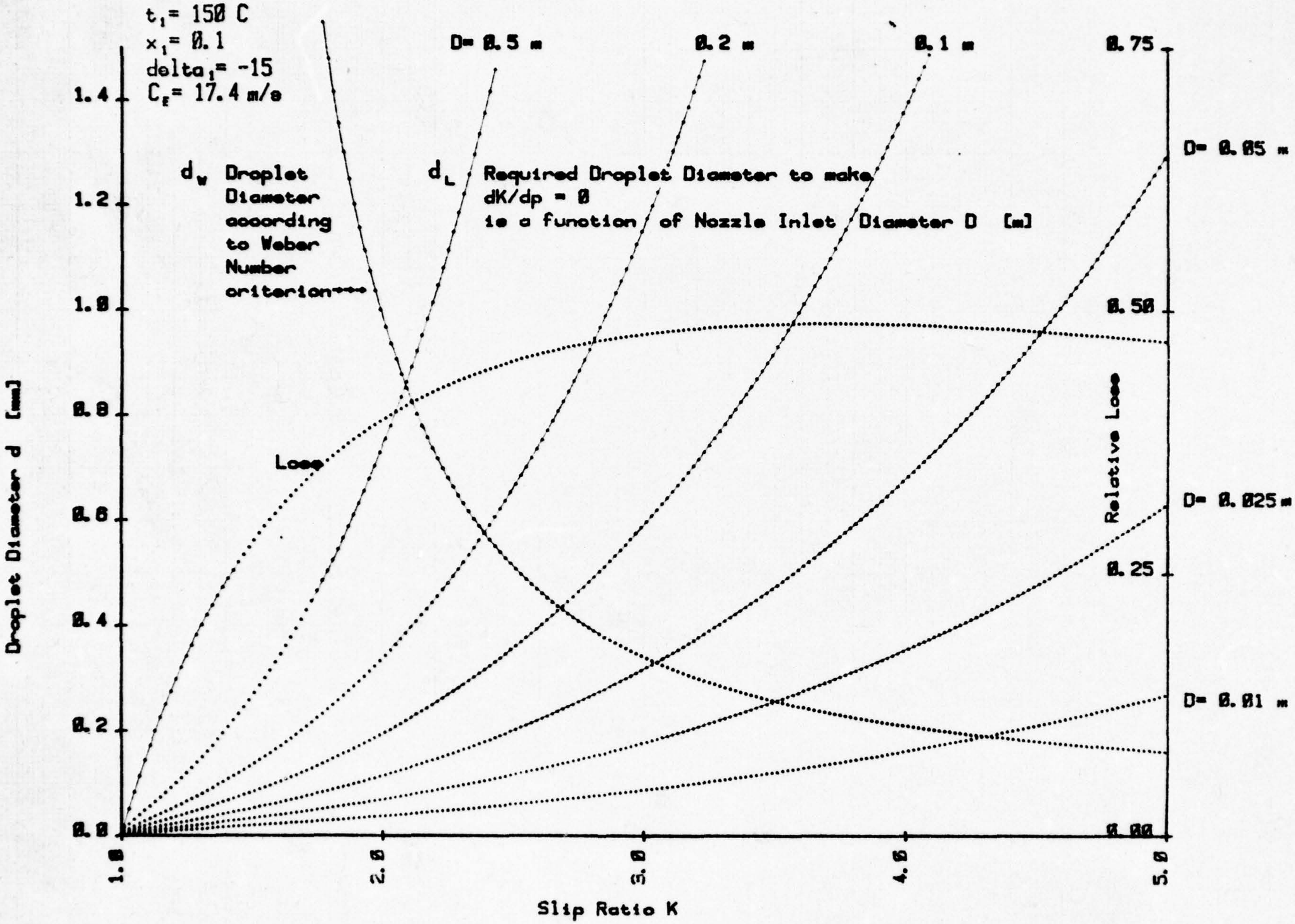

Figure 2. Initial Conditions for t_1 = 150°C

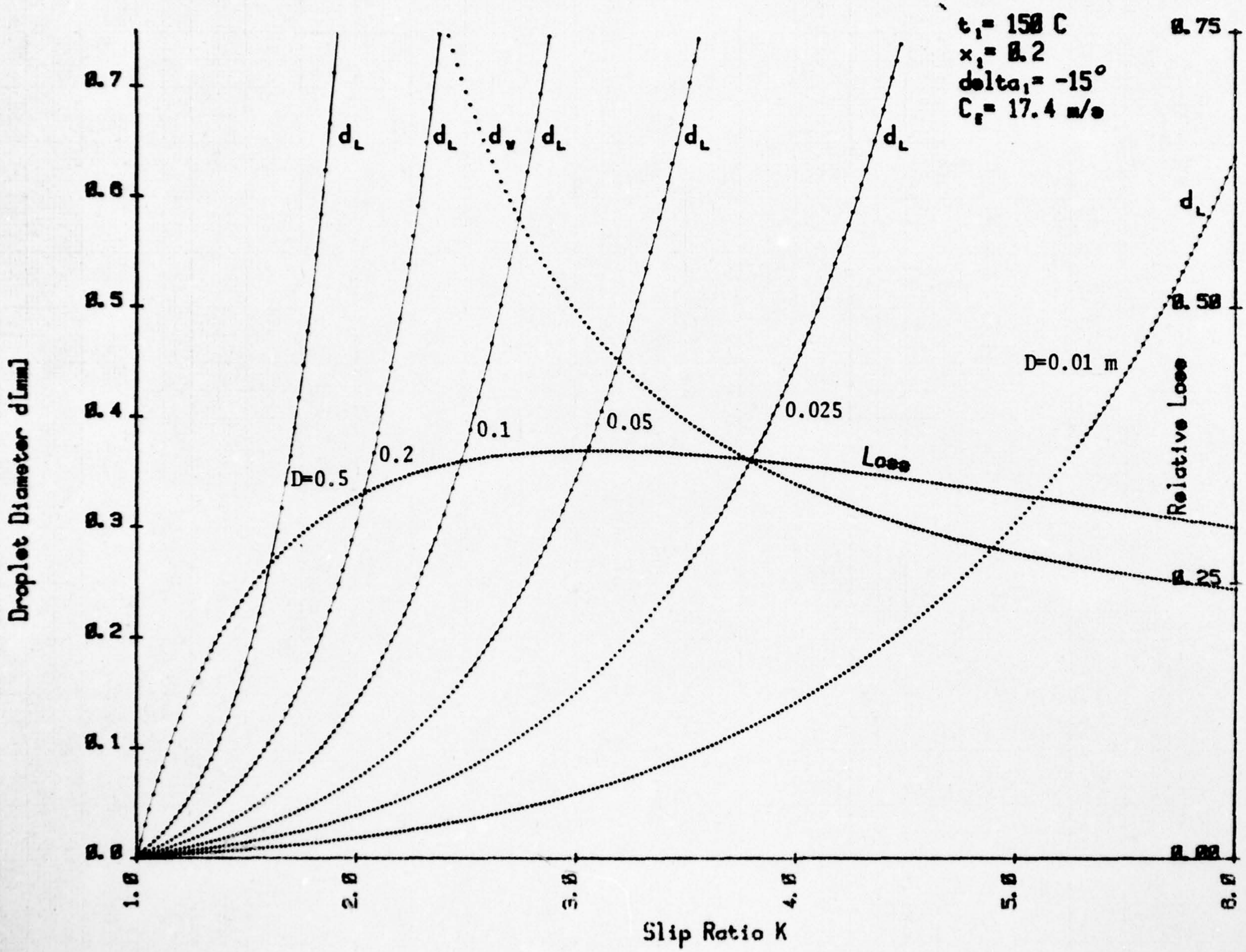

Figure 3. Initial Conditions for x_1 = 0.2

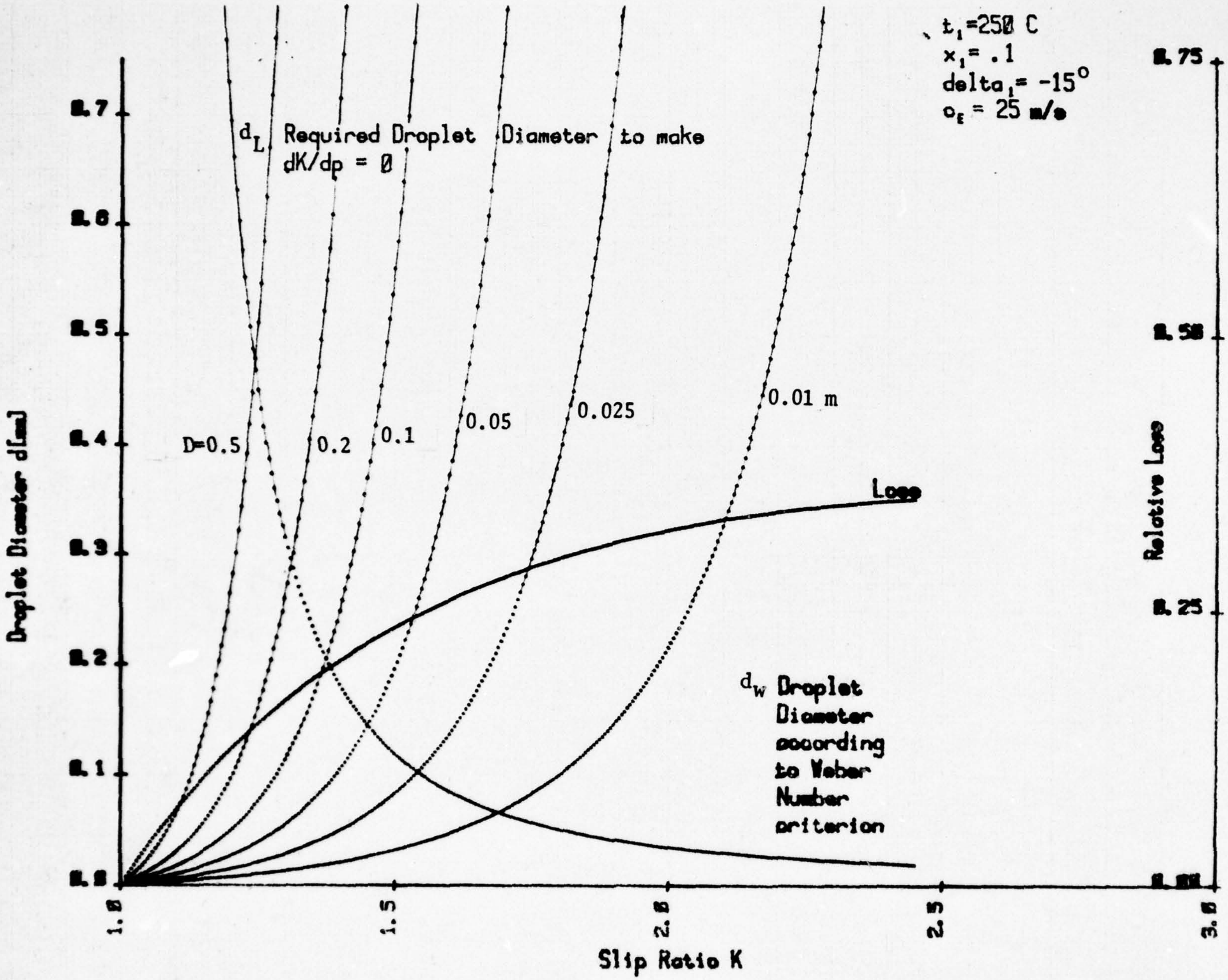

Figure 4. Initial Conditions for t_1 = 250°C

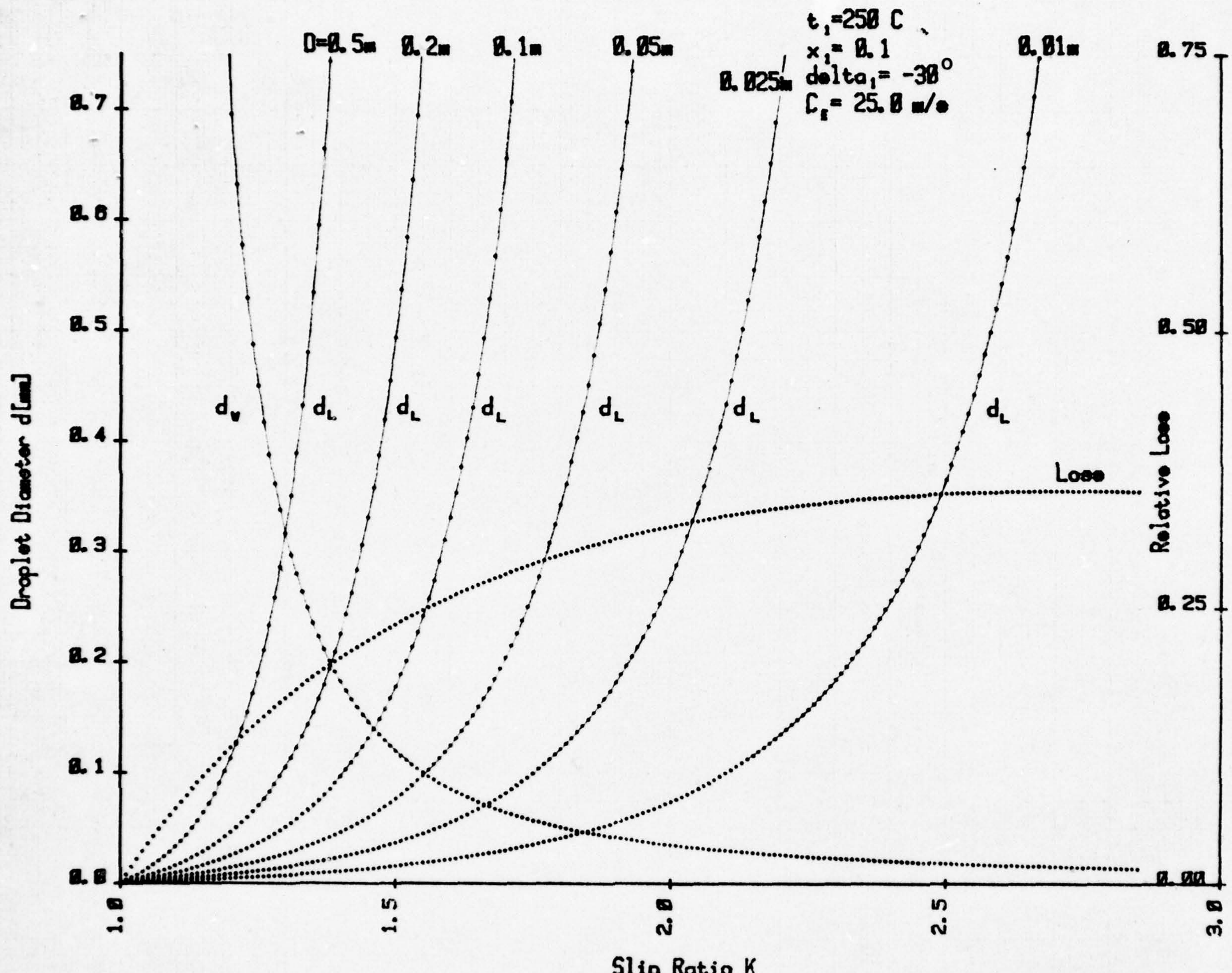

Figure 5. Initial Conditions for δ_1 = -30°

The Throat Conditions

The throat is located at the plane of maximum mass-flux density $\dot{m}/A$. At the same time the local relative losses should reach their minimum at the throat. Since the relative loss $1 - \eta_N$ is proportional to the product WS, the slope at the wall, tan δ, cancels out, so that a discontinuity can be tolerated by the one-dimensional theory. Since the axial length increment dx^* is theoretically zero at a sharp throat, the loss should accordingly be zero. That requires the pressure gradient dp/dx^* to tend toward infinity, see Eq. (73).

In an actual program execution it was initially found difficult to maintain the accuracy required to achieve coincidence at one and the same temperature of the two events of maximum mass-flux density on one hand, maximum gradient and minimum efficiency on the other hand. The difficulty was attributed to the effect of $C_E{}^2/2$, (that is, the value by which the local enthalpy differs from the value at stagnation conditions). The effect of C_E is explicitly present in the differential Eq. (90), as well as implicitly through the presence in W, see Eq. (96).

A refined equation for dK/dp was first developed, based upon the assumption of a negligible effect on droplet size of a varying relative velocity at the droplet over the axial extent of an element. Next the influence of a varying C_E was considered everywhere else and was algebraically eliminated. Further details were already given in connection with the quadratic Eq. (101) for $C_E{}^2$.

The question is whether the peak in mass-flux density $\dot{m}/A$ can be accurately determined when $\dot{m}/A$ depends on W, and the value of W should be adjusted according to its definition - Eq. (82), to the changing tan δ at the throat (from the value in the converging part to the value in the diverging part).

The answer is that if $(1 - \eta_N) \to 0$ at the throat, Eq. (58) for dK/dp may be resorted to, which is entirely general, (the loss mechanism being represented solely by $(1 - \eta_N)$ in one of the terms). Since a change in tan δ at the throat only affects the loss formulation, a negligible loss situation is made independent of δ and is represented by Eq. (58) with $(1 - \eta_N) \to 0$, that is

$$\frac{dK}{dp} + \frac{(1-\hat{x})}{2x(1-x)} \frac{dx}{dp} + \frac{K}{C_E^2} \hat{x} \left(\frac{v_a}{K} - Kv_b \right) = 0 \tag{122}$$

For lower values of x and moderate K values we have $(1-\hat{x}) > 0$, and $dx/dp < 0$. The third term is always positive when $v_a >> v_b$, and much larger than the second term of Eq.(122). As a result dK/dp is generally negative, that is, the slip increases at the throat. That is borne out by actual computer runs.

The other relation that has to be met at the throat is Eq. (73), which represents the reciprocal of the normalized pressure gradient. With the pressure gradient tending towards infinity, S becomes zero.

If the temperature (or pressure) and the vapor fraction is assumed as known at the throat, the enthalpy difference $C_E^2/2$ may be calculated from Eq.(73) for an assumed slip ratio K as follows:

$$\boxed{C_E^2 = \frac{\hat{x}\left(\frac{v_a}{K} - Kv_b\right) - \frac{2\hat{x}\bar{v}}{\bar{x}V}}{\frac{\hat{x}-1}{2x(1-x)} \frac{dx}{dp} + \frac{2R}{V}}} \quad (S = 0) \tag{123}$$

where

$$R = Z \frac{dx}{dp} + \frac{x}{\bar{v}\sqrt{K}} \frac{dv_a}{dp}$$

$$Z = \frac{\left(\sqrt{K} - \frac{1}{\sqrt{K}}\right)}{\bar{x}} + \frac{\frac{v_a}{\sqrt{K}} - v_b\sqrt{K}}{\bar{v}}$$

$$V = \frac{x\sqrt{K} - \frac{1}{\sqrt{K}}}{\bar{x}} - \frac{\frac{xv_a}{\sqrt{K}} - (1-x)v_b\sqrt{K}}{\bar{v}}$$

were given before.

A check may be obtained for Eq. (123) by setting conditions for single phase operation with an ideal gas as follows:

<u>For K = 1.0 (no slip)</u>:

$$\hat{x} \to 1.0 \ , \quad \bar{x} \to 1.0 \ , \quad \bar{v} \to v_m$$

$$V = 2x - 1 - [xv_a - (1-x)v_b]/v_m$$

$$Z = \frac{v_a - v_b}{v_m}$$

$$R = Z\frac{dx}{dp} + \frac{x}{v_m}\frac{dv_a}{dp} \quad .$$

<u>For a Single Phase Gas</u>:

$$x = 1$$

$$\frac{dx}{dp} = 0$$

$$v_m \to v_a \ , \quad v_b \to 0$$

$$V \to 0$$

$$Z \to 1$$

$$R = \frac{dv_a/v_a}{dp} \quad .$$

For an Ideal Gas:

$$\frac{dv}{v} = \frac{-1}{k}\frac{dp}{p}$$

so that

$$R = -\frac{1}{kp} \quad .$$

After substitution into Eq. (123) we get

$$C_E{}^2 = \frac{-v_a}{R} = \frac{-v_a}{-\frac{1}{kp}} = kpv_a \quad . \tag{124}$$

That is the square of the sonic velocity in an ideal gas.

Returning now to two-phase conditions, Eq. (123) may be programmed and results obtained as presented in Figure 6 for the variation of C_E with changing slip ratio K, and throat temperature as a parameter. Additional exploration over a wide range of K values shows that for a given temperature C_E reaches a minimum value for a certain slip ratio. Over a range of temperatures from 100 to 200°C, that minimum value changes only from about 118 m/s to 120 m/s.

Knowledge of the value of C_E and the slip ratio K at the throat (for given temperature and vapor mass fraction x) allows the calculation of the mass-flux density $\dot{m}/A$ at the throat, which is useful for the sizing of the throat for a required mass flow. Typical mass-flux densities are shown in Figure 7 for x = 0.125 and t = 100 to 150°C at the throat.

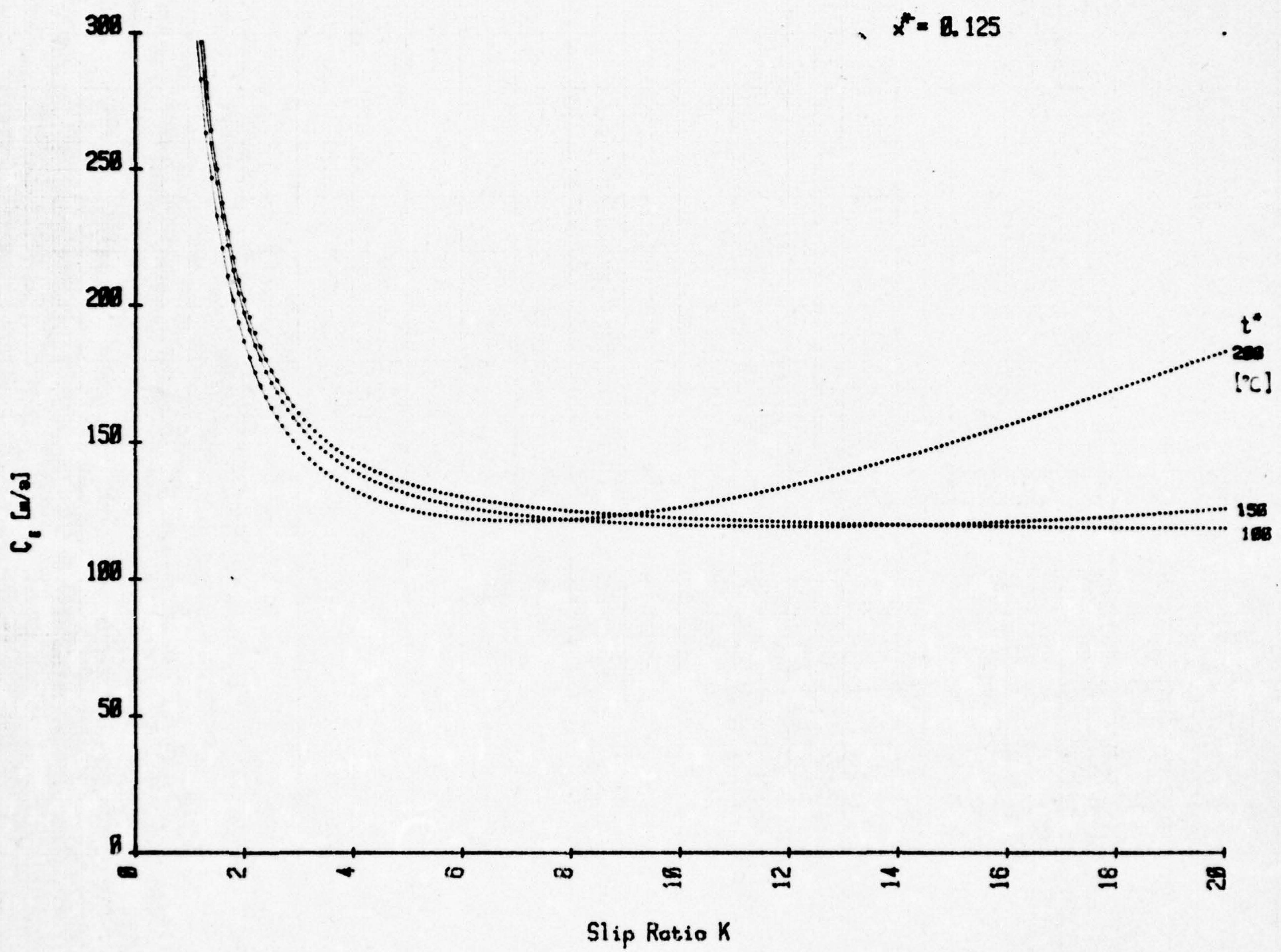

Figure 6. Throat Condition

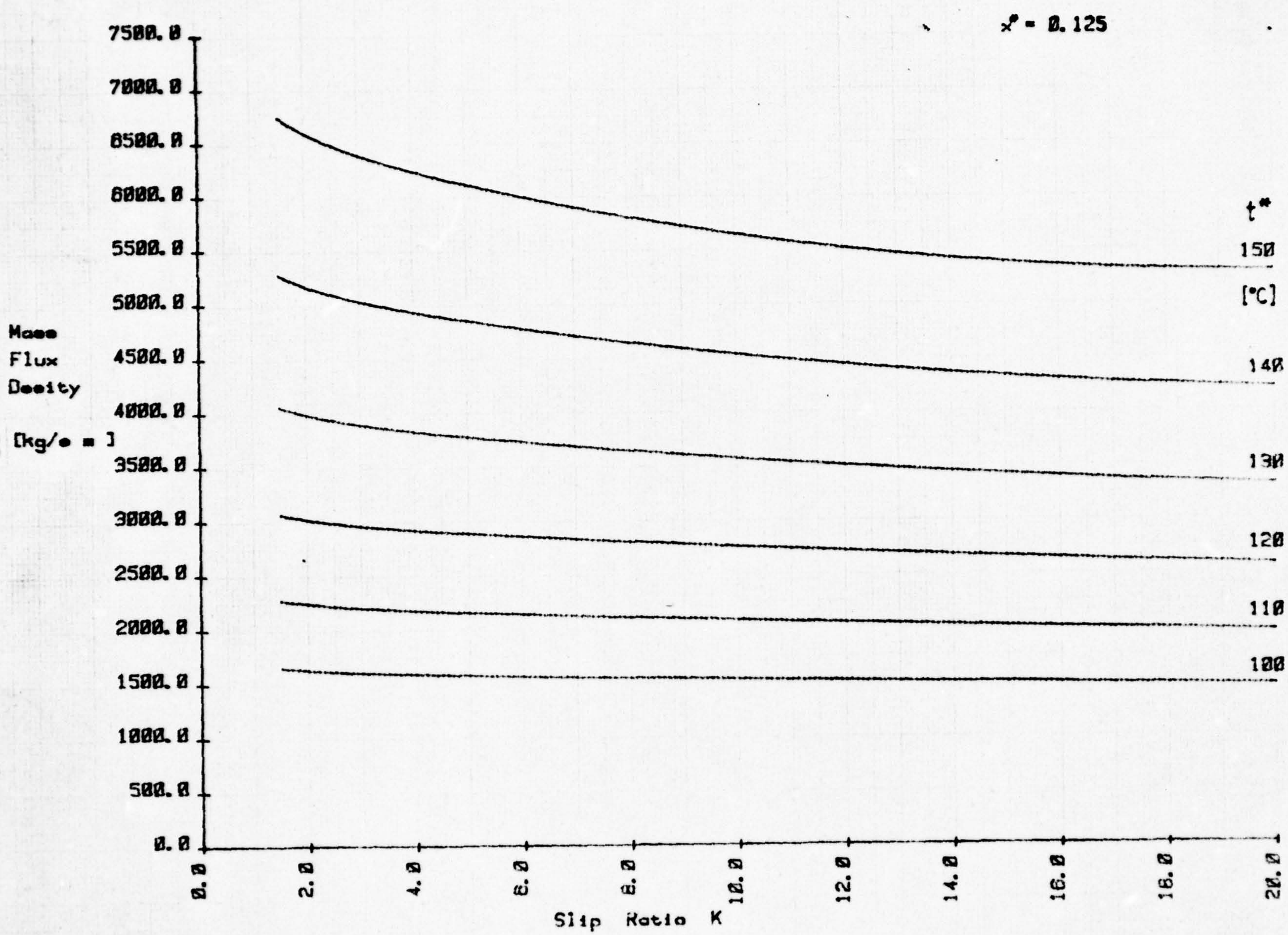

Figure 7. Throat Condition: Maximum Mass-flux Density

In Reference 4 a normalized mass-flux density

$$\phi = \dot{m}\sqrt{RT_o} / A_T p_o \tag{125}$$

was presented based upon the slip-free IHE model, and a given nozzle inlet temperature in the range from 100°C to 300°C.

Note that according to Equation (25) an increased mass-flux density at the throat is due to the ratio $v_m/\bar{v}\sqrt{K}$, which tends toward K for small x, and the speed ratio $(C_E/C_s)^*$.

It is necessary to distinguish clearly between three situations: (1) the conditions and results of the IHE model, (2) the results of the slip model at K>1, (3) the results of the slip model at K=1. A comparison of mass-flux density may be made based upon either (a) the same inlet stagnation conditions or (b) the same pressure and temperature condition at the throat. Equation (25) yields for K=1 (no slip)

$$\frac{(\dot{m}_t)_{K=1}}{(\dot{m}_t)_{IHE}} = \left(\frac{C_E}{C_s}\right)^* .$$

If the temperature at the throat and at the inlet is assumed the same for both models, the enthalpy drop should also be the same for no slip, that is $C_E^* = C_s^*$ and the results of the two models (1) and (3) should coincide for K=1.

Since Equation (123) gives a value of C_E^2 which is only dependent on the quantities t, x and K, it is not tied to a certain inlet condition t_o, except that it should not exceed C_s and therefore calls for a maximum t_o. The above assumption of equal stagnation conditions for the two models when the throat condition is the same is therefore not necessarily justified, and

larger mass-flux densities are possible for the slip model when the throat conditions are reached at a lower enthalpy than for the IHE model (starting from the same stagnation enthalpy).

The curves for C_E of Figure 6 show a strong increase of C_E towards lower slip ratios K. Its influence on mass-flux density seems to override the effect of the first factor of Equation (25), since Figure 7 shows the highest mass-flux density at small slip ratios. Since C_E is only weekly dependent upon temperature, according to Figure 6, the question of how the mass-flux densities compare for the two models, based upon identical stagnation conditions may have to be answered by actual computer runs for both, the IHE model and the slip model (in order to locate the throat).

From a series of such computer runs it was borne out that the limiting values of C_E and $\dot{m}/A$ given in Figures 6 and 7 are closely approached if the local efficiency is high. Low local efficiencies near the throat are, however, possible if the pressure gradient is low. Throat values of C_E and $\dot{m}/A$ are then much lower than the limiting values given.

A basic question touched upon is that of the value of the sonic velocity at the throat in a two-phase mixture with slip. For further details see References 6, 9 and 14

The limiting value of C_E given as a function of K allows also the determination of a minimum droplet size as a function of K that may be expected at the throat and thereafter. Figure 8 shows such results. It is seen that values of d of the order of a few microns are possible if high local efficiencies near the throat are realized.

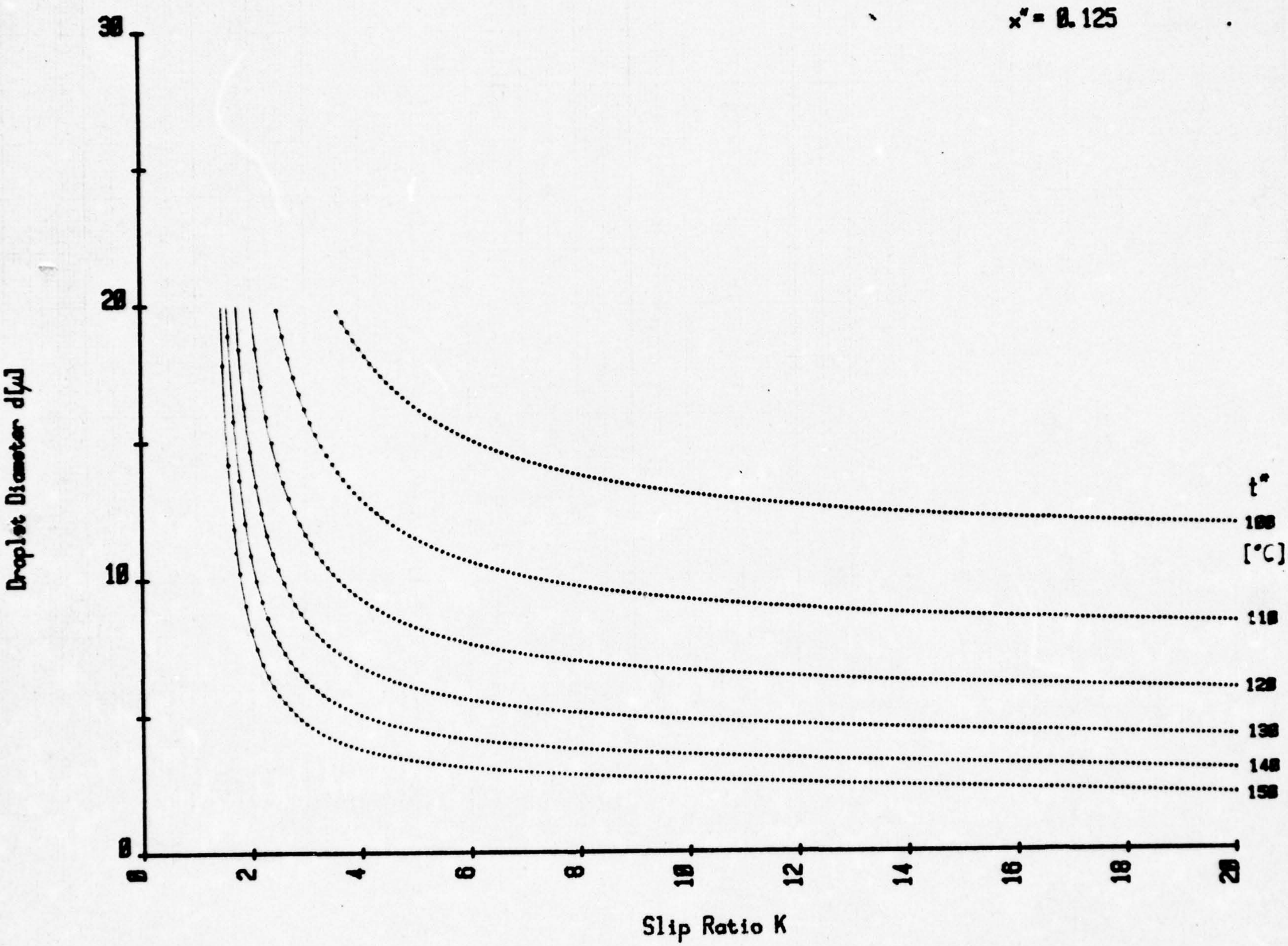

Figure 8. Throat Condition: Minimum Droplet Size

Experience With Running The Computer Program for the Nozzle Expansion

The program was systematically debugged; the results of the subroutine for the properties of wet steam were checked against tabular values, until the deviations were a fraction of one per cent. For the viscosity of saturated steam the latest international standards were initially used; in order to reduce the program running time a formula of the form of *SUTHERLAND's* was selected and the two constants adjusted such that close agreement with the "International Formula" was achieved, see Appendix II.

Most running experience was obtained with $150^{o}C$ inlet temperature, an initial vapor mass fraction of $x=0.1$, an initial velocity C_E of 17.4 m/s, and a very small nozzle inlet diameter of 0.01 m (see Figure 9). Without preatomization, the Weber Number criterion gives an initial droplet size (for $dK/dp=0$) of 190 μm, and an initial slip ratio of $K=4.30=C_a/C_b$. It climbs initially when using $\delta= -15^{o}$ =constant over the converging part. The slip ratio thereafter decreases and reaches a minimum of $K=4.05$ at about $143^{o}C$ and then increases again towards the throat, where it reaches a value of $K=5.70$ at a temperature of $126.5^{o}C$. The vapor fraction at the throat is 0.1399, the mass-flux density $\dot{m}/A=3202.2$ kg/sm², the droplet size $d=11.6$ μm, the velocity C_E corresponding to the enthalpy change $C_E=141.7$ m/s, the throat diameter $D=5.702$ mm and an S-value of $S=1.60 \times 10^{-8}$ m²/N. A sharp transition from one cone angle to another of opposite sign is permissible at the throat; the K curve will then show a discontinuity of the derivative, whereas the efficiency and the gradient S will experience step changes. As the angle δ changes its sign, W will also change sign from positive to negative, and S will change sign from plus to minus.

While the normalized inverse of the pressure gradient, S, may be used to calculate the diameter change for a certain temperature

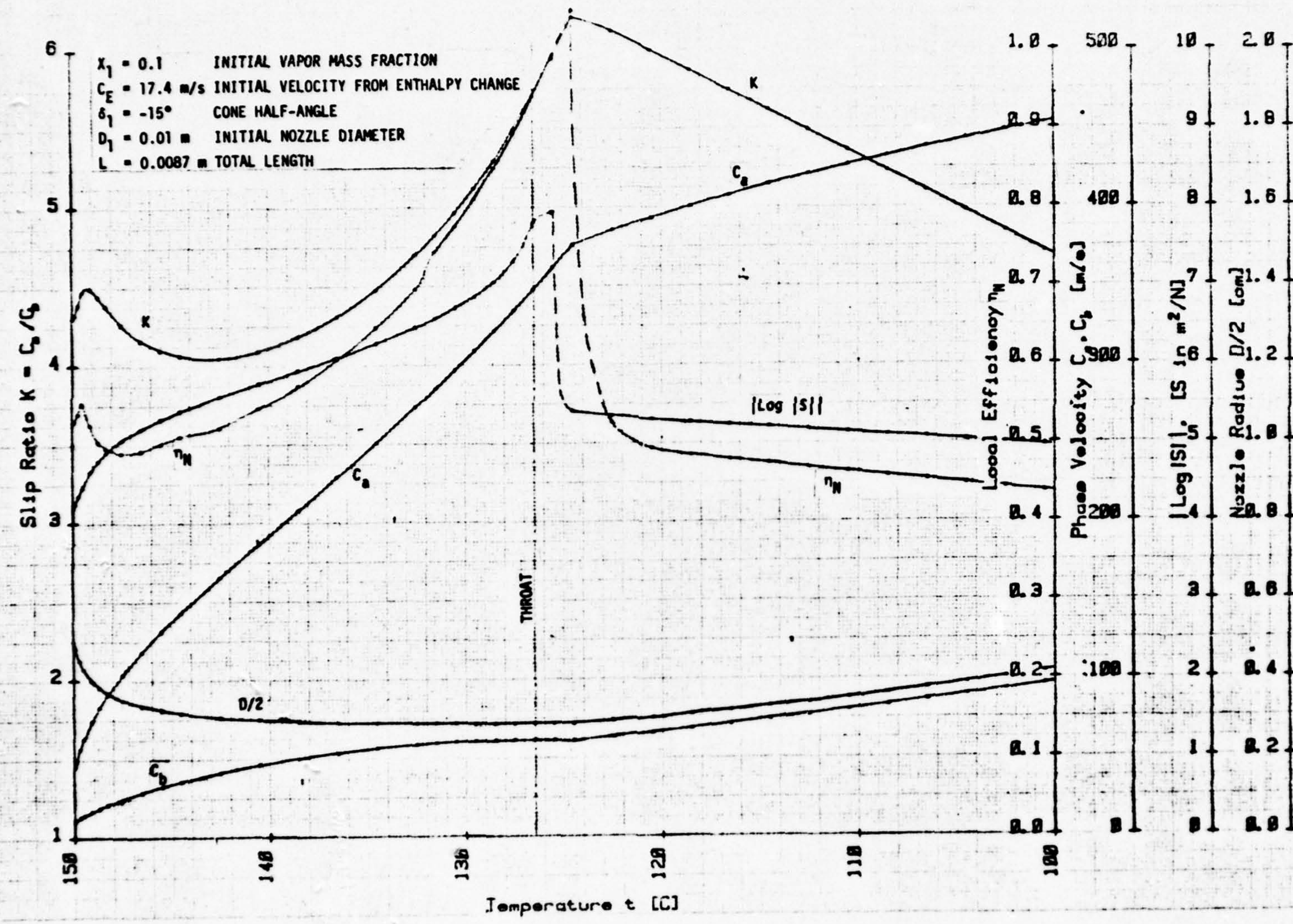

Figure 9. Expansion in a Short, Small Two-Phase Nozzle (With Conical Converging Section), Without Preatomization

or pressure change, it is more accurate to calculate the mass-flux density from Equation (23) at each inlet to an elementary step, and use its ratio across a step to determine the area ratio required. Still, the quantity S gives an indication of the diameter changes and the local efficiency potential.

Near the throat, S tends to be very small and the pressure changes are large for a given temperature change.

In the diverging part of the nozzle, a negative S should increase in its absolute value in order to allow the expansion to proceed with smaller and smaller pressure changes (for given uniform temperature changes). At the same time the losses are bound to increase according to Equation (83).

For very small nozzles (of the order of 0.5 cm throat diameter) the slip ratio was large, and orderly expansion in the diverging part was found difficult to obtain with a simple straight cone geometry. The program, however, allows changing the cone angle δ at every elementary step such that a compromise in the variation of S and η_N is obtained.

With a prescribed fixed cone angle in the diverging part of the nozzle, the situation was encountered where a negative S would increase in absolute value with progressing expansion. While the mass-flux density was still decreasing from step to step, the pressure changes were large, the efficiency was rising, and eventually, when S was allowed to change sign from the normal negative to a positive sign, the pressure gradient would reverse and the efficiency would reach unity at the same point. Within the constraints of the prescribed equation system, which does not make allowance for the occurrence of shocks, only an increase in cone angle δ downstream of that point could avert the physically untenable condition of a rising pressure linked to a prescribed falling temperature. The limiting condition as described,

gradually develops when the absolute value of S has been decreasing steadily, which means that for uniform steps of temperature the diameter increase and therefore the axial movement of the state point along the nozzle has become less and less. That condition benefits the local efficiency because the drag work becomes less and less, until (when S changes sign and goes through zero) the losses go to zero when the axial displacement dx^* has ceased to develop. Obviously, at this point no further regular expansion is possible: the selected cone angle δ is insufficient to accommodate an increasing volume flow. The above development goes parallel with a steadily increasing slip ratio K.

A guideline for the required cone angle δ may be obtained by solving for W while dK/dp of Equation (90) has a prescribed increasing value (dK<0). The equation for W_δ becomes accordingly

$$W_\delta = \frac{Q\left\{\frac{dK}{dp} + K\left[\frac{1-\hat{x}}{2x(1-x)}\frac{dx}{dp} + \frac{\hat{x}}{C_E^2}\left(\frac{v_a}{K} - Kv_b\right)\right]\right\}}{\frac{1}{2}\bar{x}\hat{x}V\, dK/dp + K(\hat{x}^2\bar{v}/C_E^2 + \bar{x}\hat{x}R)} \tag{126}$$

The cone angle δ required follows from Equation (82). Use of Equation (126) in the program leads to an automatic calculation of the required nozzle geometry that will give a prescribed slip ratio slope at the inlet to each nozzle element.

Such a sample solution is given in Figure 10.

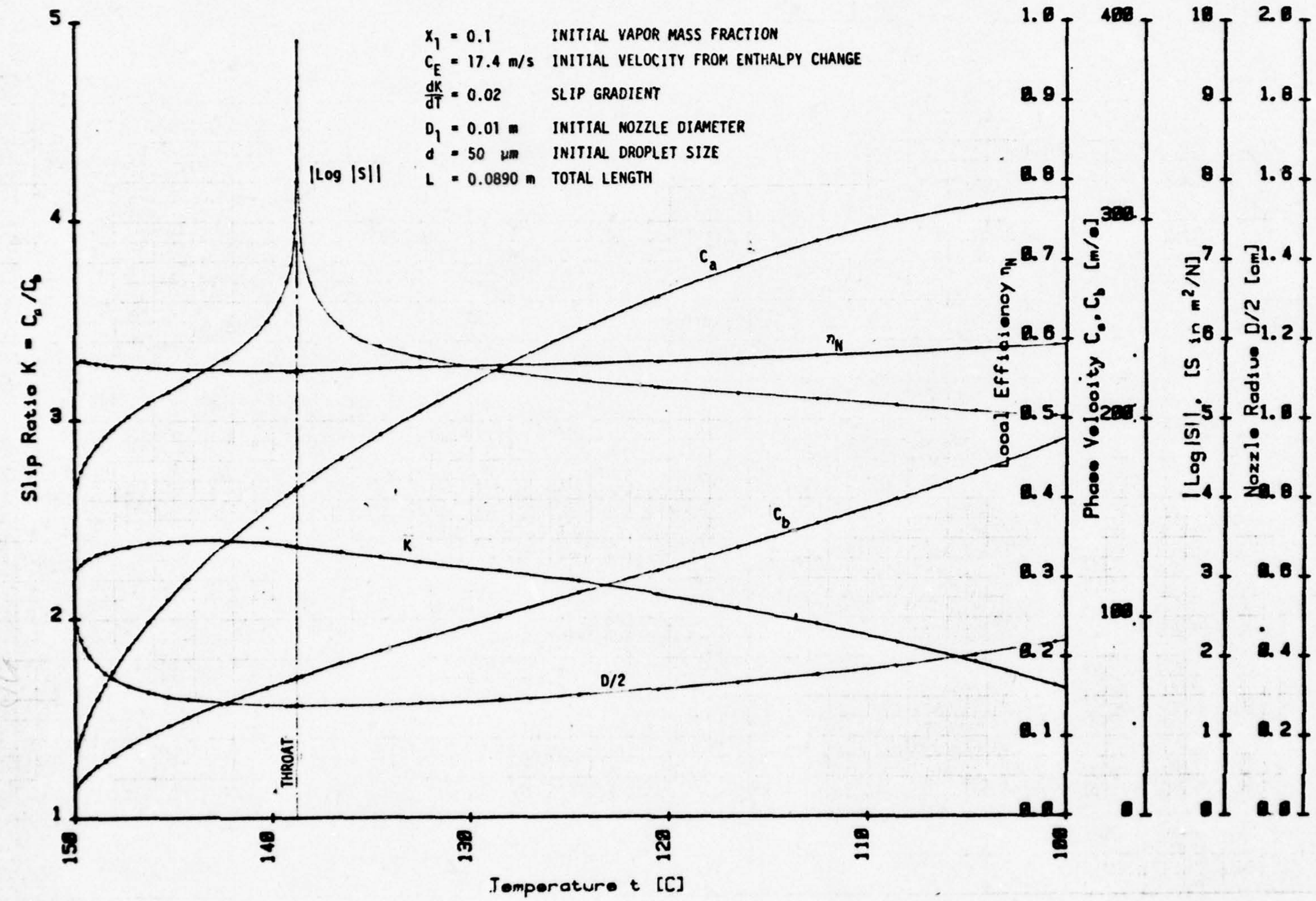

Figure 10. Expansion of Wet Steam in a Small Convergent-Divergent Nozzle With Preatomization

PART II

DROPLET TRAJECTORIES IN A TURBINE PASSAGE

In a cylindrical coordinate system (r,Θ,z) the material derivative is (C_r = radial, C_u = peripheral velocity components of the droplet)

$$\frac{D}{Dt} = \frac{\partial}{\partial t} + C_r\frac{\partial}{\partial r} + \frac{C_u}{r}\frac{\partial}{\partial \Theta} + C_z\frac{\partial}{\partial z} \quad . \tag{127}$$

The projections a_r, a_u, a_z of the acceleration vector of a liquid droplet in the coordinate directions are

$$\begin{aligned} a_r &= \frac{DC_r}{Dt} - \frac{C_u{}^2}{r} \\ a_u &= \frac{DC_u}{Dt} + \frac{C_r C_u}{r} \\ a_z &= \frac{DC_z}{Dt} \quad . \end{aligned} \tag{128}$$

If we neglect the force due to the pressure gradient in the passage, the buoyancy and mass changes of the droplet, the aerodynamic drag is the only remaining force with the drag coefficient C_D

$$D = C_D A \rho_a \frac{C\vec{C}}{2} \quad . \tag{129}$$

Using the mass of a spherical droplet

$$m = \rho_b \frac{\pi}{6} d^3 \tag{130}$$

and equating D to $m\vec{a}$ we get

$$\vec{a} = \frac{3}{4} \frac{C_D}{d} \frac{\rho_a}{\rho_b} |C| \vec{C} \quad . \tag{131}$$

Equating the individual components we obtain

$$\frac{DC_r}{Dt} = \frac{C_u{}^2}{r} + \frac{3}{4} \frac{C_D}{d} \frac{\rho_a}{\rho_b} |C| C_r$$

$$\frac{DC_u}{Dt} = -\frac{C_r C_u}{r} + \frac{3}{4} \frac{C_D}{d} \frac{\rho_a}{\rho_b} |C| C_u \tag{132}$$

$$\frac{DC_z}{Dt} = \frac{3}{4} \frac{C_D}{d} \frac{\rho_a}{\rho_b} |C| C_z \quad .$$

Such a set of equations was solved for the two-dimensional case ($C_z = 0$) in Reference 15 by numerical integration. Unfortunately insufficient information is given there for generalizing the results.

A simple analysis of droplet trajectories was developed in Reference 4. The result will be given by the ratio of the radial drift velocity w_b of the droplets in relation to the steam velocity C. A flow angle deviation of the droplets from the steam is thereby given.

Since considerable analysis was applied to the study of the processes in the nozzle (because they form the foundation of what is to happen thereafter in the turbine) the criteria developed in Reference 4 will be repeated here, together with some sample calculations.

The *relative velocity* between droplet and steam in radial direction is designated as w_b and needs to be calculated.

The drag force on the droplet of diameter d is defined by

$$D = C_D \frac{1}{v_a} \frac{w_b{}^2}{2} \frac{\pi}{4} d^2 \quad , \tag{133}$$

where v_a is the specific volume of the surrounding medium. The drag coefficient C_D is given as a function of Reynolds number $Re = w_b\, d/v_a$ in Figure 11 according to a relation given in Reference 7 which is valid for $0.1 < Re < 20{,}000$: [See also Eq. (88).]

$$\ln C_D = 3.271 - 0.8893 \ln Re + 0.03417(\ln Re)^2 + 0.001443(\ln Re)^3$$

Since the slip velocity w_b is not initially known for the calculation of Re and C_D, the quantity $Re\sqrt{C_D}$ was plotted against Re in Figure 12 , since $Re\sqrt{C_D}$ is expressible in terms of known values as follows.

The inertia force on a spherical droplet of diameter d and specific volume v_b that travels with velocity C on an initially assumed circular path of radius of curvature, r_k, is

$$F = \frac{1}{v_b} \frac{\pi d^3}{6} \frac{C^2}{r_k} \quad . \tag{134}$$

Corrected for buoyance B we get

$$F - B = \frac{1}{v_b} \frac{\pi d^3}{6} \frac{C^2}{r_k} \left(1 - \frac{v_b}{v_a}\right) \quad . \tag{135}$$

Equating the two forces of Equations (133) and (135) gives

$$\frac{w_b}{c} = \sqrt{\frac{4}{3} \frac{d}{r_k} \frac{1}{C_D} \left[\frac{v_a}{v_b} - 1\right]} \quad . \tag{136}$$

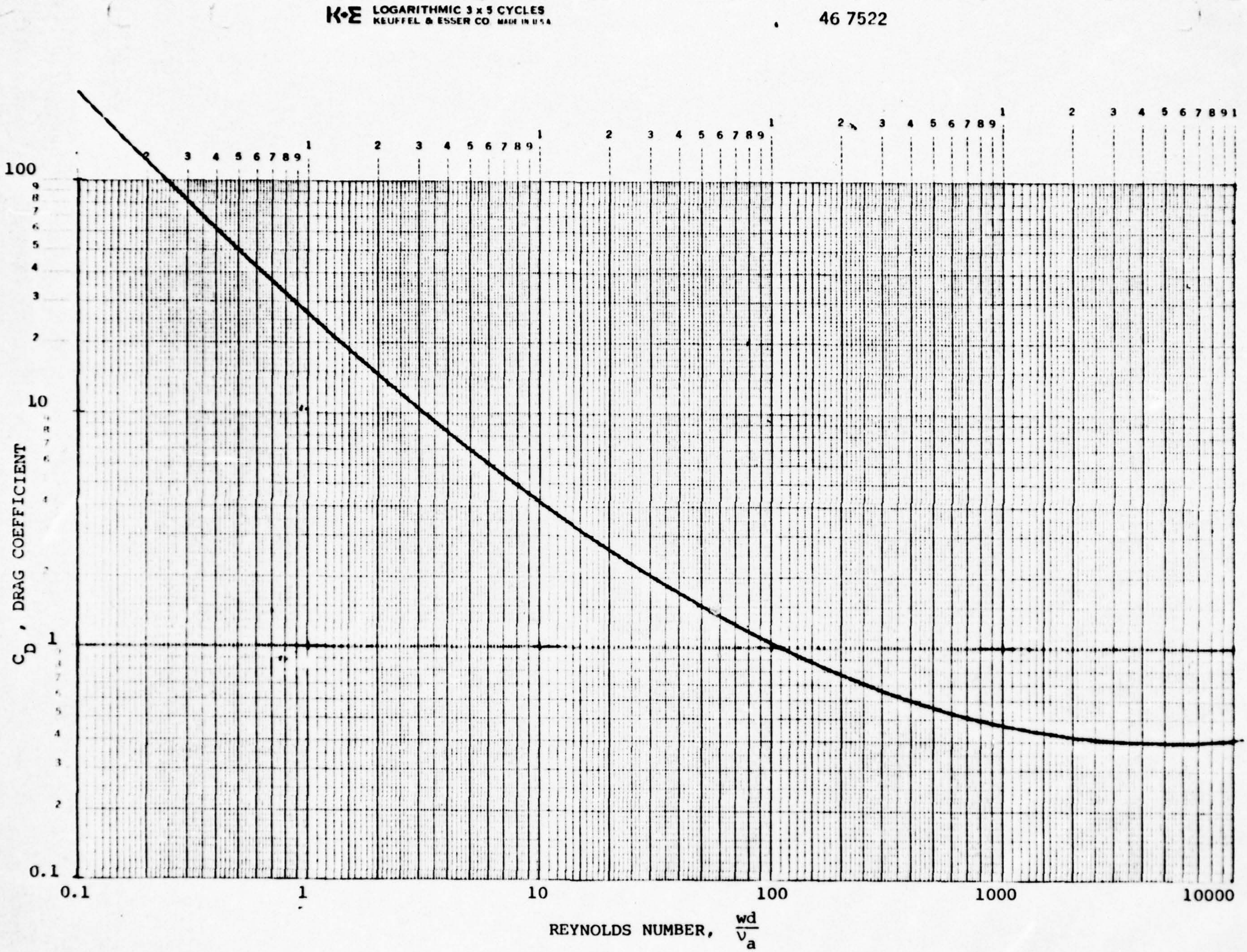

Figure 11. Drag Coefficient of Spherical Droplets

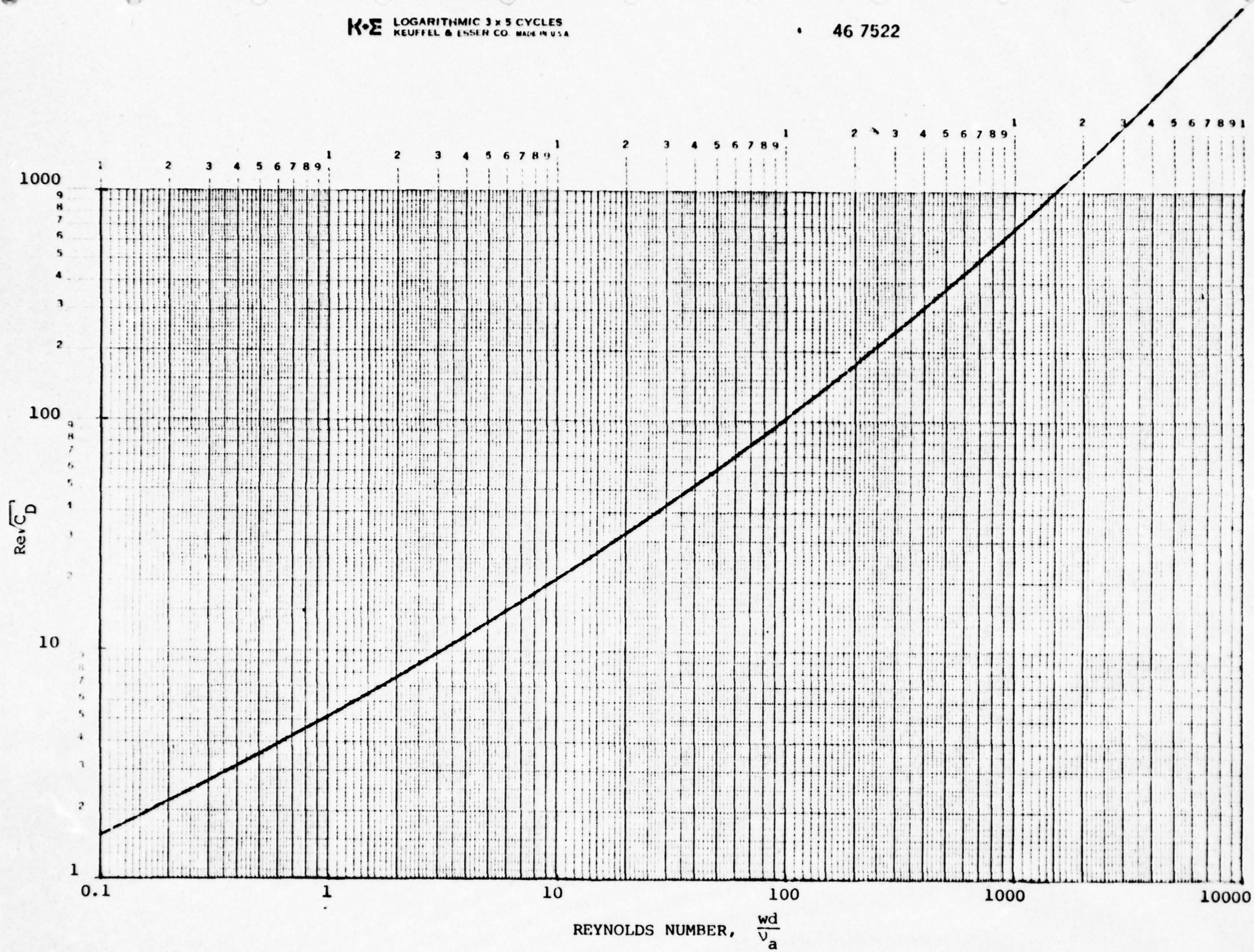

Figure 12. Working Graph for Determining Slip Velocity of Spherical Droplets for a Given Diameter

It is convenient to refer velocities to the reference velocity $e = \sqrt{p\, v_a}$ and lengths to the mean free path length

$$\lambda_a = \frac{v_a \eta_a}{e} \quad . \tag{137}$$

Accordingly

$$Re = \frac{w_b}{e} \frac{d}{\lambda_a}$$

and (139)

$$Re\sqrt{C_D} = \frac{w_b}{C} \sqrt{C_D} \frac{C}{e} \frac{d}{\lambda_a}$$

$$= \frac{C}{e} \sqrt{\frac{4}{3} \frac{d}{r_k} \left(\frac{d}{\lambda_a}\right)^2 \left[\frac{v_a}{v_b} - 1\right]} \quad .$$

Therefore, the proof is furnished that the quantity $Re\sqrt{C_D}$ is solely composed of known quantities, namely the droplet diameter d, the vapor property λ_a, the ratio of specific volumes v_a/v_b, the radius of curvature of the path, r_k, and the normalized absolute velocity C/e (∿ Mach number) along the path. Entering Figure 12 on the ordinate will yield Re and consequently the desired w_b/e from (138)

$$\frac{w_b}{e} = \frac{Re}{d/\lambda_a} \quad . \tag{140}$$

Equation (139) shows that the expression $Re\sqrt{C_D}$ is a function of the relative droplet velocity C/e in the path with radius of curvature r_k. The resulting relative slip velocity w_b/e is a

measure of the deviation from the original path. For this purpose the ratio w_b/C is significant and may be used for a step by step trajectory analysis.

An illustrative example might be helpful. Assume an absolute pressure of steam of 0.250 bar that corresponds to a saturation temperature of 65°C. Accordingly

$$\frac{v_a}{v_b} = \frac{6.206}{10^{-3}} = 6206$$

$$e = \sqrt{p\,v_a} = 393.9 \text{ m/s}$$

$$\lambda_a = \frac{v_a \eta_a}{e} = \frac{6.206 \text{ x } 1.065\text{x}10^{-5}}{393.9} = 1.678 \text{ x } 10^{-7} \text{ m}$$

$$d = 2 \text{ μm}$$

$$\frac{d}{\lambda_a} = 11.919$$

$$r_k = 10 \text{ cm} = 0.1 \text{ m}$$

$$C = 250 \text{ m/s}$$

$$\frac{C}{e} = 0.635 \quad .$$

Equation (139) yields

$$Re\sqrt{C_D} = \frac{C}{e}\sqrt{\frac{4}{3}\,\frac{d}{r_k}\left(\frac{d}{\lambda_a}\right)^2\left[\frac{v_a}{v_b} - 1\right]} = 3.0772 \quad .$$

From Figure 12: $Re = 0.46$

and $$\frac{w_b}{e} = \frac{Re}{d/\lambda_a} = \frac{0.46}{11.919} = 0.0386$$

or $$\frac{w_b}{C} = \frac{0.0386}{0.635} = \underline{0.0608} ,$$

or an angle deviation of 3.5^o.

If the droplet size is diminished to 1 μm the result is

$$Re\sqrt{C_D} = 1.0885$$

$$Re = 0.06$$

$$w_b/e = \frac{0.06}{5.96} = 0.0101$$

$$w_b/C = 0.0159$$

$$\alpha = 0.908^o$$

It is seen that the deviation of the liquid droplets from the path of the steam due to drift is small for such small droplet sizes and a radius of curvature of 10 cm, see Figure 13.

To summarize, the non-dimensional parameters which control the droplet trajectories in the turbine are

$\frac{C}{e}$ the Mach index of the steam flow ,

$\frac{d}{r_k}$ the ratio of droplet size to the radius of curvature of the path in the bucket ,

$\frac{d}{\lambda_a}$ the ratio of droplet diameter to the mean free path length of the molecules in the steam,

$\frac{v_a}{v_b}$ the specific volume ratio of steam to liquid .

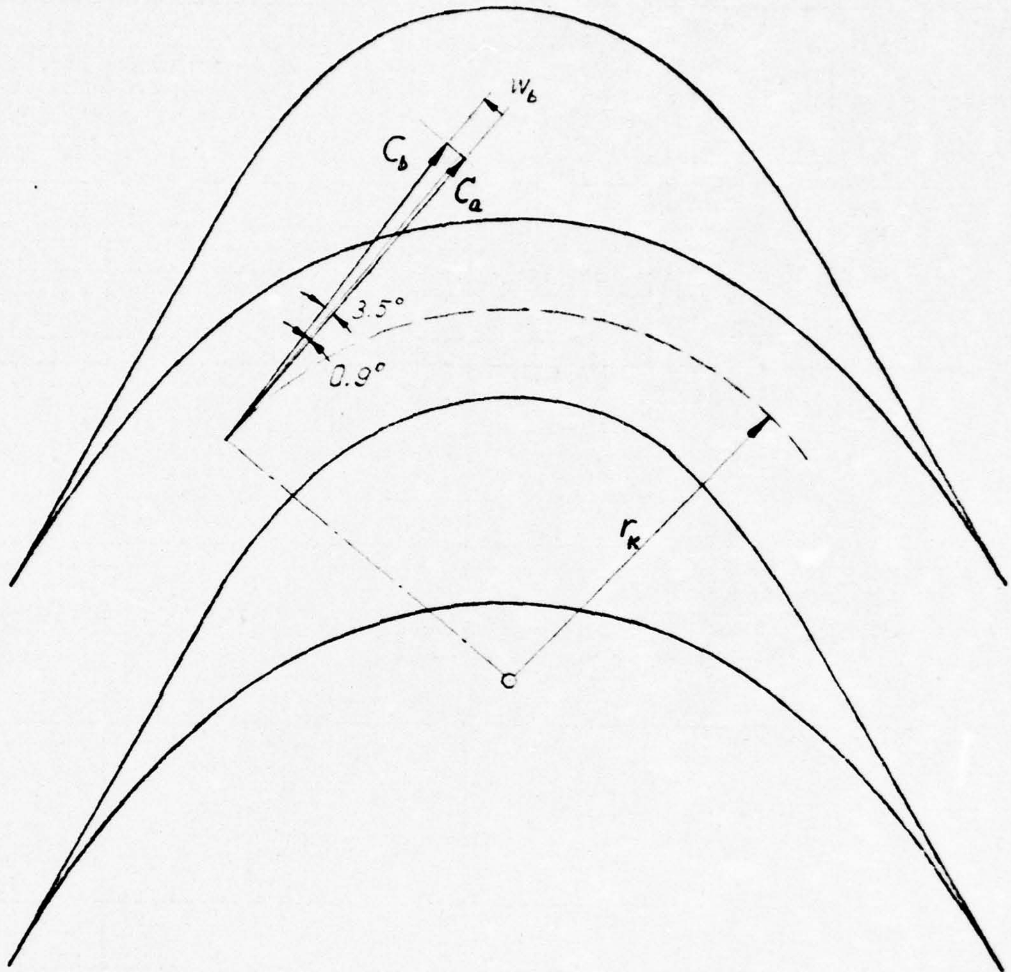

Figure 13. Deviations of Droplet Velocities From Steam Velocities in an Impulse Bucket

The smaller $Re\sqrt{C_D}$, the smaller Re, and therefore

$$\frac{w_b}{e} = \frac{Re}{d/\lambda_a} \quad .$$

The lower the specific volume v_a of the steam, the lower the droplet deviation w_b/e. For $Re \leq 0.1$ the simple Stokes formula is valid

$$C_D = \frac{24}{Re} \quad . \tag{141}$$

Therefore,

$$Re\sqrt{C_D} = \sqrt{24\,Re}$$

and after substitution into Equation (139) we get

$$\frac{w_b}{C} = \frac{w_b/e}{C/e} = \frac{Re}{(C/e)(d/\lambda_a)}$$

$$= \frac{1}{18}\ \frac{C}{e}\ \frac{d}{r_k}\ \frac{d}{\lambda_a}\left[\frac{v_a}{v_b} - 1\right] \quad . \tag{142}$$

The normalized deviation w_b/C in the Stokes regime is proportional to droplet diameter squared, the Mach index $C/\sqrt{p\,v_a}$, the ratio v_a/v_b (if $v_a \gg v_b$) and inversely proportional to the product $r_k\lambda_a$. For further discussion see "Conclusions and Recommendations".

CONCLUSIONS AND RECOMMENDATIONS

Two areas of two-phase flow were considered: (a) the one-dimensional flow of wet steam in a converging-diverging nozzle, (b) the two-dimensional flow through impulse turbine buckets.

A theory based upon a simple model was developed for the nozzle problem, which is a foundation for the turbine problem.

Both the slip ratio K and the droplet size d at the nozzle discharge are needed for the solution of the turbine problem. To determine the slip ratio, a proven local relative-loss model was used to express the frictional drag losses between droplets and steam, while the droplet size was established by limiting the value of the Weber number to six.

Expressions for the mass-flux density, vapor and liquid velocities, droplet size, thrust and overall nozzle efficiency have been included. These relationships have been solved numerically by a digital computer.

The results predict an increased mass-flux density is to be expected in the presence of slip for mixtures of low vapor mass fractions compared to the prediction of the IHE model. In addition, the model indicates that larger slip ratios do not necessarily mean large losses and, hence, low local efficiencies, although this is generally the case for the overall efficiency.

In the absence of preatomization, purely algebraic considerations establish the initial slip ratio and droplet size at the nozzle inlet. If, on the other hand, the droplet size is predetermined by means preceding the nozzle, the corresponding initial slip ratio can also be determined algebraically.

The ratio of the nozzle and droplet diameters is predicted to increase as the nozzle diameter increases, which results in a higher nozzle performance. For a given nozzle size, smaller

droplets (below the Weber threshold) result in lower values of slip and local losses if $K < 2.5$.

In the development of the computer program for the step-wise nozzle expansion, entirely different situations were encountered in the converging as compared to the diverging part of the nozzle. While the assumption of a given cone angle throughout the converging portion lead to solutions without difficulties, a similar assumption for the diverging part would be acceptable for a certain portion, but would eventually lead to a tie-up of further expansion (within the constraints of the formulations used, like continuous expansion, no shock waves admitted).

By allowing a change in the cone angle δ along the axis, which means a departure from the straight cone geometry, orderly expansion can be obtained. The choice of the angle, however, is critical since too small an angle leads to poor local efficiencies (coupled with a drop of the slip ratio K and a decrease of the value of the pressure gradient and an increase in droplet size d.

Since the behavior of K, η and pressure gradient is interrelated, it is possible to find a suitable nozzle contour (or cone angle δ) by prescribing a certain gradient dK/dT at the inlet of each step. A solution obtained for a small nozzle is shown in Figure 10 where dK/dT was uniformly equal to 0.02 at the beginning of each step.

The investigation of two-phase flow in an impulse turbine was necessarily brief and is given in Part II. The results given at the end of Part II show that the relative deviation of the droplets from the steam path will increase with the Mach index of the steam flow, the ratio of droplet diameter to the radius of curvature of the flow in the turbine bucket and the ratio of droplet diameter to the "mean free path length of the steam molecules". Also, the larger the specific volume of the steam, the larger the droplet flow deviation. Combining the mean-free path

length with the other steam conditions gives for the "Stokes Regime"

$$w_b/C_a = \frac{1}{18} \frac{C_a\ d^2}{v_b \eta_a r_k} \quad ,$$

which has the form of a Reynolds Number, with d^2/r_k as reference length. To minimize droplet impingement on the buckets, a large radius of curvature r_k of the flow path is needed, together with low steam velocities and small droplet diameters. Even with droplet impingement and liquid film formation, acceptable performance seems possible with dished radial outward buckets as were proposed in Reference 8.

Further studies are required, especially with larger machine dimensions. Systematic applications of the computer programs developed should give nozzle designs of the characteristics required for high performance machines. That conclusion is supported by the results of Reference 7.

Arabic

a	Acceleration
A	Cross-sectional area of nozzle
A^*	Throat area of nozzle
$C'_a = C''$	Specific heat of saturated steam
$C_b = C'$	Specific heat of saturated water
C	Index for independent variable
C_a	Velocity of steam
C_b	Velocity of water droplets
C_D	Drag coefficient
C_E	$\sqrt{2(i_{m_o} - i_m)}$
C_S	Velocity from isentropic expansion
d	Droplet diameter
D	Nozzle diameter
D_F	Droplet drag
$e = \sqrt{pv}$	Reference velocity
H	Index for successive discretizations
i	Static enthalpy
i_m	Static enthalpy of mixture
I	Index in solution matrix T[J,I]
J	Index in solution matrix T[J,I]

NOMENCLATURE

K	C_a/C_b slip ratio
L	Power loss
$\dot{m}$	Mass flow
$\dot{m}_T$	Total mass flow
N[H]	Number by which step size is divided by
p	Static pressure
Q	$4x(1-x)(\sqrt{K} - 1/\sqrt{K})$
r_c	Latent heat of evaporation
r_k	Radius of curvature of path
R	$Z\ dx/dp + \frac{x}{\bar{v}\sqrt{K}} \frac{dv_a}{dp}$
Re	Reynolds number $dw/v_a \eta_a$
s	Entropy
S	2dD/Ddp
t	Temperature [°C]
T	Temperature [°K]
v	Specific volume
v_m	Specific volume of mixture
$\bar{v}$	$\frac{xv_a}{\sqrt{K}} + (1-x)v_b\sqrt{K}$
V	$\frac{x\sqrt{K} - \frac{(1-x)}{\sqrt{K}}}{\bar{x}} - \frac{\left[\frac{xv_a}{\sqrt{K}} - (1-x)v_b\sqrt{K}\right]}{\bar{v}}$

NOMENCLATURE

w Relative velocity between droplet and steam

W $-\frac{3}{2} C_D \frac{(1-x)}{\hat{x}} \frac{v_b}{v_a} \frac{(K-1)^3}{K} \frac{D}{d \tan \delta}$

We $\frac{w^2 d}{2 v_a \sigma}$

x Vapor mass fraction (quality)

x^* Axial length coordinate of nozzle

$\hat{x}$ $xK + (1-x)/K$

$\bar{x}$ $x\sqrt{K} + (1-x)/\sqrt{K}$

Y[C,H] Dependent variable, approximation of

Z $\frac{\sqrt{K} - \frac{1}{\sqrt{K}}}{\bar{x}} + \frac{\left(\frac{v_a}{\sqrt{K}} - v_b\sqrt{K}\right)}{\bar{v}}$

Greek

α Static void fraction

δ Half angle of conical nozzle element

η_a Viscosity of steam

η_N Nozzle efficiency (local and overall)

λ_a $v_a \eta_a / e$ "Mean free path length of steam molecules"

ρ Mass density

σ Surface tension

NOMENCLATURE

(Page 4 of 4)

Subscripts and Superscripts

0	Stagnation conditions
1	Nozzle inlet
a	Steam
b	Liquid
*	Throat conditions

REFERENCES

1. STARKMAN, E.S., SCHROCK, V.E., NEUSEN, K.F. and MANEELY, D.J., "Expansion of a Very Low Quality Two-Phase Fluid Through a Convergent-Divergent Nozzle", Trans ASME, Journal of Basic Engineering, June 1964, page 247-256.

2. KEENAN, J.H., "Thermodynamics", Wiley, Inc., N.Y., 1941.

3. STODOLA, A., and LOEWENSTEIN, L.C., "Steam and Gas Turbines" Volume I and II, Peter Smith, N.Y., 1945.

4. HAYS, L. and RITZI, E., "Design Study of a Two-Phase Turbine Engine for Submarine Propulsion", Final Report to ONR, N-00014-77-C-0545, Biphase Energy Systems, Inc., Santa Monica, CA, August 18, 1978.

5. DZUNG, L.S. and GYARMATHY, G., "Critical Mass Flux Density in Two-Phase Flow", Brown Boveri Review, Volume 65, Number 1, January 1978, Baden, Switzerland, page 55-61.

6. DZUNG, L.S. "Thermostatische Zustandsänderungen des trockenen und des nassen Dampfes", Zeitschrift für Angewandte Mathematik und Physik, Volume 6, 1955 (3), page 207-223.

7. ELLIOTT, D.G. and WEINBERG, E., "Acceleration of Liquids in Two-Phase Nozzles", Technical Report 32-987, Jet Propulsion Laboratory, Pasadena, CA, July 1968.

8. RITZI, E.W., "Design Study of a Two-Phase Turbine Engine for Torpedo Propulsion", for Naval Surface Weapons Center, N-60921-76-C-0276, Biphase Energy Systems, Inc., Santa Monica, CA, June 1977.

9. VENEDIKTOV, V.D., "Two-Phase Flow in Turbines and Reaction Nozzles", Moscow, 1969, Translation NASA TT F-613.

10. HINZE, J.O., "Critical Speeds and Sizes of Liquid Globules", Applied Scientific Research, "Delft" Laboratory, Royal Dutch Shell, Volume A1, 1947, page 273-288.

11. BULIRSCH, R. and STOER, J., "Numerical Treatment of Ordinary Differential Equations by Extrapolation Methods". Numerische Mathematik, Volume 8, (1966), page 1-13.

12. RANDOLPH, H.L., "Numerical Analysis Handbook", McDonnell Douglas Automation Company, Huntington Beach, CA, December 1975.

13. BULIRSCH, R. and STOER, J., "Fehlerabschätzung und Extrapolation mit Rationalen Funktionen bei Verfahren vom Richardson-Typus". Numerische Mathematik, Volume 6, (1964), page 413-427.

14. RADOVSKIY, I.S., "Speed of Sound in Two-Phase Vapor-Liquid Systems", Heat Transfer-Soviet Research, Volume 3, Number 3, May-June 1971, page 104-112.

15. KIRILLOV, I.I. and YABLONIK, R.M., "Fundamentals of the Theory of Turbines Operating on Wet Steam", Leningrad, 1968, Translation NASA TT F-611.

16. PLANK, R., "Thermodynamische Grundlagen" Handbuch der Kältetechnik, Volume II, Springer, Göttingen, 1953.

17. HENDRICKS, R.C., McCLINTOCK, R.B., and SILVESTRI, G.J., "Revised International Representations for the Viscosity of Water and Steam and New Representations for the Surface Tension of Water", Trans ASME, Journal of Engineering for Power, October 1977, page 664 - 678.

APPENDIX I

BIBLIOGRAPHY

Subjects

(1) Erosion and Corrosion
(2) Droplets and Atomization
(3) Flow Studies

Literature

Listed chronologically with author, title, source, and date.

Subject

1.(1) Fraas, A.P., "Survey of Turbine Bucket Erosion, Deposits, and Corrosion", *American Society of Mechanical Engineers*, Paper No. 75-GT-123, August 12, 1975.

2.(1) Habercom, Guy E., Jr., "Turbine Blades: Corrosion and Erosion (A Bibliography with Abstracts)", *National Technical Information Service*, NTIS/PS-75/127, January 1975.

3.(3) Evans, D.H. and W.D. Pouchot, "Flow Studies in a Wet Steam Turbine", *National Aeronautics and Space Administration*, Report No. NASA CR-134683, August 13, 1974.

4.(1) Pouchot, W.D. and others, "Basic Investigation of Turbine Erosion Phenomena", Final Report, *Westinghouse Astronuclear Laboratory*, WANL-TME-1977, January 1971.

5.(3) Dzung, L.S. and G. Gyarmathy, "Critical Mass Flux Density in Two-Phase Flow", *Brown Boveri Review 1*, January 1978.

6.(1) Heymann, F.J., "Erosion by Liquids", *Machine Design*, December 10, 1970, pp. 118-124.

7.(2) Farmer, R. and others, "Liquid Droplet Deposition in Two-Phase Flow", *Journal of Heat Transfer - Transaction of the ASME*, November 1970, pp. 587-594.

8.(2) Wiegand, H., *On the Break-up of a Liquid Jet in a Sequence of Uniform Size Liquid Droplets*, Technical Translation of DLR FB 67-31, Deutsche Forschungs-und Versuchsanstalt für Luft-und Raumfahrt, June 1970.

9.(3) Soo, Shao L. and others, "Measurement of Mass Flow and Density of Aerosols in Transport", *Environmental Science and Technology*, Vol. 3, April 1969, pp. 386-393.

10.(1) Hays, L.G., *Third Stage Material Loss Calculations*, October 1968.

11.(2) Varljen, Thomas C., "The Transport of Atomized Drops in Wet Vapor Turbines", *Westinghouse Astronuclear Laboratory*, WANL-TME-1836, August 5, 1968.

12.(1,2) Varljen, T.C. and C.M. Glassmire, "Estimation of Moisture Formation and Deposition and of the Threshold for Turbine Bucket Erosion in Potassium and Cesium Vapor Turbines", *Westinghouse Astronuclear Laboratory*, WANL-PR(CCC)-004, January 1968.

13.(2) Varljen, T.C., "Calculation of Trajectories of Atomized Drops in Wet Vapor Turbines", *Westinghouse Astronuclear Laboratory*, WANL-TME-1711, December 20, 1967.

Subject

14.(1) Westinghouse Astronuclear Laboratory, *Basic Investigation of Turbine Erosion Phenomena*, Progress Reports, January 1967 - March 1969.

15.(1,2) Sanders, W.P., *Water Droplet Formation and Flow Leading to Bucket Erosion in Steam Turbines*, presented at Western Zone Meeting, Canadian Electrical Association, March 1967.

16.(1) Hays, L.G., ed., *Summary of Turbine Erosion Meeting*, held at Jet Propulsion Laboratory, December 29-30, 1966, June 15, 1967.

17.(1) Pouchot, W.D. and others, "Assembly of Analytical Model of Wet Vapor Turbine Blade Erosion", Volume 1, *Westinghouse Astronuclear Laboratory*, WANL-PR-(DD)-014, November 1, 1966.

18.(1) Pouchot, W.D. and others, Volume 2.

19.(1) Pouchot, W.D. and others, Volume 3.

20.(2) Woffinden, G.J., "Investigation of the Coalescence of Water Drops", Final Report, *U.S. Army Electronics Command*, Tech. Report ECOM-00497-2, April 1966.

21.(3) Marchik, E.A., "Motion of Condensed Phase in the Blade Passages of an Axial Gas Turbine Stage", *Thermal Engineering*, Vol. 12, 1965, pp. 63-70.

22.(1) Heymann, F.J., *Report on a Trip to Great Britain to Attend a Symposium and Visit Laboratories Concerned with the Erosion of Solids by Liquid Impact*, Westinghouse Electric Corporation, June 28, 1965.

23.(1) Loshkarev, A.I., "Erosive Abrasion Theory of the Blade Apparatus of Centripetal Turbines", *Defense Documentation Center Defense Supply Agency*, AD632-675, February 1, 1965.

24.(2) Cheng, Sin-I and Y. Rimon, "Particle Impingement on a Nozzle Wall", *Princeton University - Department of Aeronautical Engineering*, Report 696, July 1964.

25.(2) Pfeiffer, Albert, "Rebound of Liquid Drops From a Solid Surface", *U.S. Army Chemical Research and Development Laboratories*, Technical Report CRDLR 3220, July 1964.

26.(2) MacDonald, A.N., "Measuring Water Droplet Sizes in Steam", *Central Electricity Research Laboratories*, May 6, 1964.

27.(2) Wolfe, H.E. and W.H. Andersen, "Kinetics, Mechanism, and Resultant Droplet Sizes of the Aerodynamic Breakup of Liquid Drops", *Aerojet-General Corporation*, Report No. 0395-04(18)SP, April 1964.

Subject

28.(3) Gyarmathy, Georg, "Foundations of a Theory of the Wet-Steam Turbine", *Air Force Systems Command - Foreign Technology Division*, FTD-TT-63-785, April 30, 1964.

29.(2) Hanson, A.R. and others, "Shock Tube Investigation of the Breakup of Drops by Air Blasts", *The Physics of Fluids*, Volume 6, Number 3, August 1961, pp. 1070-1080.

30.(1) Gardner, G.C., "Events Leading to Erosion in the Steam Turbine", *Proc. Instn. Mech. Engrs. 1963-64*, Volume 178, Part 1, Number 23, February 26, 1963, pp. 593-623.

31.(2) Mayer, Ernest, "Theory of Liquid Atomization in High Velocity Gas Streams", *ARS Journal*, December 1961, pp. 1783-1785.

32.(2) Gretzinger, James and W.R. Marshall, Jr., "Characteristics of Pneumatic Atomization", *A.I.Ch.E. Journal*, June 1961.

33.(2) Engel, Olive G., "Collisions of Liquid Drops with Liquids", *National Bureau of Standards*, Technical Note 89, May 1961.

34.(2) Wigg, L.D., "Drop Size Prediction for Twin-Fluid Atomizers", *National Gas Turbine Establishment*, Memo. No. M.343, September 1960.

35.(3) Eisner, H.S. and others, "The Stabilization of Water Mists by Insoluble Monolayers", *Ministry of Power - Safety in Mines Research Establishment*, June 17, 1960.

36.(2) Martlew, D.L., "The Distribution of Impacted Particles of Various Sizes on the Blades of a Turbine Cascade", *National Gas Turbine Establishment*, pp. 104-111.

37.(2) Rabin, E. and others, "Displacement and Shattering of Propellant Droplets", Final Summary Report, *Rocketdyne*, R-2431, March 1960.

38.(2) Gordon, G.D., "Mechanism and Speed of Breakup of Drops", *Journal of Applied Physics*, Volume 30, Number 11, November 1959, pp. 1759-1761.

39.(2,3) Mozharov, N.A., "An Investigation into the Critical Velocity at which a Moisture Film Breaks Away From the Wall of a Steam Pipe", *Teploenergetika*, 1959 (2) 50-53.

40.(2) Ryley, D.J., "Analysis of Polydisperse Aqueous Spray from a High-Speed Spinning Disk Atomizer", *British Journal of Applied Physics*, Vol. 10, April 1959.

Subject

41.(2) Ryler, D.J., "Experimental Determination of the Atomising Efficiency of a High-Speed Spinning Disk Atomiser", *British Journal of Applied Physics*, Vol. 10, February 1959, pp. 93-97.

42.(2) Weiss, Malcolm A. and Charles H. Worsham, "Atomization in High Velocity Airstreams", *ARS Journal*, April 1959, pp. 252-259.

43.(2) Fraser, R.P. and Paul Eisenklam, "Liquid Atomisation and the Drop Size of Sprays", *Trans. Instn. Chem. Engrs.*, Vol. 34, 1956, pp. 294-318.

44.(2) Hinze, J.O., "Fundamentals of the Hydrodynamic Mechanism of Splitting in Dispersion Processes", *A.I.Ch.E. Journal*, Vol. 1, No.3, pp.289-295.

45.(2) Telford, J.W. and others, "The Coalescence Between Small Water Drops", *Commonwealth Scientific and Industrial Research Organization*, January 14, 1955.

46.(2) Marshall, W.R., Jr., *Atomization and Spray Drying*, American Institute of Chemical Engineers, New York, New York, 1954.

47.(2) Pilcher, J. Mason, *Particle Size Distribution and Concentration of Aerosols*, Letter Reports, August 10, 1954 - March 7, 1955.

48.(2) Dorsch, Robert G. and others, "Impingement of Water Droplets on an Ellipsoid with Fineness Ratio 5 in Axisymmetric Flow", *National Advisory Committee for Aeronautics*, NACA-TN-3099.

49.(2) Lane, W.R., "Shatter of Drops in Streams of Air", *Industrial and Engineering Chemistry* 43, Part 1, 1951, pp. 1312-1317.

50.(2) Kolmogorov, A.N., *The Breaking Up of Droplets in a Turbulent Stream*, Associated Technical Services, Inc., East Orange, New Jersey, 1949.

51.(2) Swinbank, W.C., "Collisions of Cloud Droplets", *Nature*, No. 4051, June 21, 1947, pp. 849-850.

52.(2) Merrington, A.C. and E.G. Richardson, "The Break-up of Liquid Jets", *The Physical Society*, Vol. 59, Part 1, No. 331, January 1, 1947.

APPENDIX II

PROPERTIES OF WET STEAM
UP TO 250°C

1. The Callendar Equation of State

The Callendar equation of state was used

$$v_a = \frac{RT}{p} - 0.075 \left(\frac{273.2}{T}\right)^{10/3} + v_b \ , \tag{II-1}$$

where T is in degrees Kelvin, and the specific volume in m³/s.

2. The Change in Vapor Specific Volume

The change in dv_a is

$$dv_a = \left(\frac{\partial v_a}{\partial T}\right)_p dT + \left(\frac{\partial v_a}{\partial T}\right)_T dp \ . \tag{II-2}$$

From Eq. (A1) the partial derivatives are as follows

$$\left(\frac{\partial v_a}{\partial T}\right)_p = \frac{R}{p} + 0.075 \ \frac{10}{3} \left(\frac{273.2}{T^2}\right) \left(\frac{273.2}{T}\right)^{7/3} , \tag{II-3}$$

and

$$\left(\frac{\partial v_a}{\partial p}\right)_T = - \frac{RT}{p^2} \ . \tag{II-4}$$

The Clausius-Clapeyron Eq. (60) gives the required dp/dT

$$\frac{dp}{dT} = \frac{r_c}{T(v_a - v_b)} , \qquad (11\text{-}5)$$

so that we get finally

$$\frac{dv_a}{dp} = \left(\frac{\partial v_a}{\partial T}\right)_p \frac{dT}{dp} + \left(\frac{\partial v_a}{\partial p}\right)_T \qquad (\text{II-2}')$$

or

$$\frac{dv_a}{dT} = \left(\frac{\partial v_a}{\partial T}\right)_p + \left(\frac{\partial v_a}{\partial p}\right)_T \frac{dp}{dT} . \qquad (\text{II-2}'')$$

3. Saturation Pressure, Latent Heat, Enthalpy and Entropy of Liquid

The remainder of the relations required was compiled from Ref. 16 and with exception of the specific heats, is summarized in Table II-1. Single primed quantities represent saturated water properties; double primed quantities represent saturated steam properties.

4. Specific Heat of Saturated Water and Steam

The specific heat of the saturated liquid is calculated using V. Regnault data, see Ref. 16, page 227

$$c_b = 4186(1 + 4\text{x}10^{-5}t + 9\text{x}10^{-7}t^2) \quad \frac{J}{kgK} . \qquad (\text{II-6})$$

The temperature t is to be taken in degrees Celsius.

The specific heat of the saturated vapor was determined from the basic equations of thermodynamics as follows

$$c_a = c_p = c_{p_o} - T\int\left(\frac{\partial^2 v_a}{\partial T^2}\right)_p dp , \qquad (\text{II-7})$$

AD-A070 754 BIPHASE ENERGY SYSTEMS SANTA MONICA CA F/G 20/4

ANALYSIS OF TWO-PHASE FLOW IN NOZZLES AND TURBINE BUCKETS.(U)

JUN 79 E RITZI N00014-78-C-0649

UNCLASSIFIED 108-F NL

2 OF 2

AD A070754

END

DATE FILMED

8 -- 79

DDC

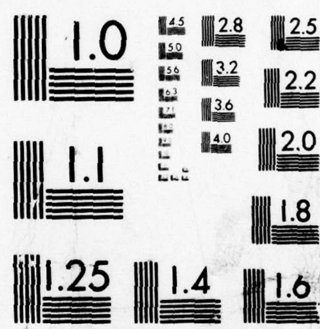

MICROCOPY RESOLUTION TEST CHART
NATIONAL BUREAU OF STANDARDS-1963-A

with $v_a = \frac{RT}{p} - C\left(\frac{273.2}{T}\right)^n + v_b$ according to Callendar, so that

$$\left(\frac{\partial^2 v}{\partial T^2}\right)_p = -C\,n(n+1)\,\frac{(273.2)^n}{T^{n+2}} ,$$

where $C = 0.075\ m^3/kg$, $n = 10/3$,

and $c_{p_o} = 1996.7\ J/kgC$,

the low pressure ideal gas specific heat of water vapor.

We finally get

$$c_a = 1996.7 + 1.0833\left(\frac{273.2}{T}\right)^{10/3} \frac{p}{T} , \qquad \text{(II-14)}$$

where the units of p are [N/m^2], and those of T in degrees Kelvin [K].

5. Calculation of dx, The Change in Vapor Mass Fraction

The total differential dx follows from

$$dx = \left(\frac{\partial x}{\partial p}\right)_s dp + \left(\frac{\partial x}{\partial s}\right)_p ds . \qquad \text{(II-15)}$$

Following Ref. (5) we get for a two-phase mixture like wet steam

$$\left(\frac{\partial x}{\partial p}\right)_s = \frac{(\partial s/\partial p)x}{(\partial s/\partial x)p} . \qquad \text{(II-16)}$$

and

$$\left(\frac{\partial s}{\partial x}\right)_p = s'' - s' , \qquad \text{(II-17)}$$

where $s'' - s'$ is the entropy change upon evaporation. Since

$$s = xs'' + (1-x)s' \tag{II-18}$$

$$\left(\frac{\partial s}{\partial p}\right)_x = x\frac{ds''}{dp} + (1-x)\frac{ds'}{dp} \; . \tag{II-19}$$

The differential ds'' is

$$ds'' = \left(\frac{\partial s''}{\partial p}\right)_T dp + \left(\frac{\partial s''}{\partial T}\right)_p dT \; . \tag{II-20}$$

For an assumed ideal gas model for the saturated vapor of specific heat c_p, the Eq. of Gibbs is

$$Tds = c_p dT - vdp \; , \tag{II-21}$$

and therefore:

$$\left(\frac{\partial s''}{\partial p}\right)_T = -\frac{v''}{T} \tag{II-22}$$

and

$$\left(\frac{\partial s''}{\partial T}\right)_p = \frac{c_p}{T} \; . \tag{II-23}$$

Use of the Clapeyron Equation

$$\frac{dp}{dT} = \frac{s'' - s'}{v'' - v'} \tag{II-24}$$

gives after substitution of Eq. (II-24), (II-22) and (II-23) into Eq. (II-20)

$$\frac{ds''}{dp} = -\frac{v''}{T} + \frac{c_p}{T}\frac{(v'' - v')}{(s'' - s')} \tag{II-25}$$

which is ready for substitution into Eq. (II-19).

For the saturated liquid of specific heat c'

$$\frac{ds'}{dp} = \frac{ds'}{dT}\frac{dT}{dp} = \frac{c'}{T}\frac{(v'' - v')}{(s'' - s')} \qquad \text{(II-26)}$$

which is to be substituted into Eq. (II-19) also.

Final substitution of Eq. (II-17) and (II-19) into Eq. (II-16)

gives
$$\left(\frac{\partial x}{\partial p}\right)_s = \frac{x(v''-v')}{T(s''-s')}\left[\frac{v_a}{(v''-v')} + \frac{c' - c_p}{(s''-s')}\right] - \frac{c'}{T}\frac{(v'' - v')}{(s' - s')^2} \qquad \text{(II-27)}$$

or

$$\left(\frac{\partial x}{\partial T}\right)_s = \frac{x}{T\left(1 - \frac{v'}{v''}\right)} + \frac{x(c' - c_p)}{r_c} - \frac{c'}{r_c} \qquad \text{(II-28)}$$

The second term in Eq. (II-15) may be written

$$\left(\frac{\partial x}{\partial s}\right)_p \frac{ds}{dp}\frac{dp}{dT}$$

From the definition of efficiency, $\eta_N = di/vdp$, we get from the Gibbs Equation, $Tds = di - vdp$,

$$1 - \eta_N = \frac{-Tds}{v_m dp} \qquad \text{(II-29)}$$

or

$$\frac{ds}{dp} = \frac{-v_m(1 - \eta_N)}{T} \qquad \text{(II-30)}$$

so that finally, from Eqs. (II-15) and (II-17)

$$\boxed{\frac{dx}{dT} = \left(\frac{\partial x}{\partial T}\right)_S - \frac{v_m(1 - \eta_N)}{T(v'' - v')}} \quad . \qquad \text{(II-31)}$$

6. Viscosity of Saturated Steam

The final formula used is of the Sutherland type, as follows

$$\eta_t = \eta_o \frac{273 + C}{T + C} \left(\frac{T}{273}\right)^{3/2} \quad , \qquad \text{(II-32)}$$

where

$$\eta_o = 8.6843 \times 10^{-6} \quad [kg/ms]$$

$$C = 498.3732 \quad [^oC]$$

$$T = \text{Temperature} \quad [^oK] \quad .$$

Sample values were calculated according to the latest international formula, see Reference 17; they are tabulated below together with results from the above formula.

VISCOSITY OF SATURATED STEAM

t [°C]	International Formula 1975 η [kg/ms]	Sutherland Formula η [kg/ms]
100	1.227760×10^{-5}	1.2285×10^{-5}
110	1.262300×10^{-5}	1.2637×10^{-5}
120	1.297068×10^{-5}	1.2987×10^{-5}
130	1.331996×10^{-5}	1.3336×10^{-5}
140	1.367034×10^{-5}	1.3684×10^{-5}
150	1.402147×10^{-5}	1.4030×10^{-5}

7. Surface Tension of Water

The "International Association for the Properties of Steam" released in September 1975 the following formula for the surface tension of water (that is valid between the triple point and the critical point)

$$\sigma = 0.2358 \left(1 - \frac{T}{647.15}\right)^{1.256} \left[1 - 0.625 \left(1 - \frac{T}{647.15}\right)\right] \qquad \text{(II-33)}$$

where T is to be given in [$^{\circ}$K], and the units of surface tension σ are [N/m], see Reference 17.

Table II-1. Saturated Steam Properties

$$\log\left(\frac{p_k}{p}\right) = \frac{\left(1 - \frac{T}{T_k}\right)}{T/T_k}\left[\frac{a+bT_k\left(1 - \frac{T}{T_k}\right) + dT_k{}^3\left(1 - \frac{T}{T_k}\right)^3 + eT_k{}^4\left(1 - \frac{T}{T_k}\right)^4}{1 + fT_k\ (1 - T/T_k)}\right] = z \qquad \text{(II-8)}$$

$p/p_k = 10^{-z}$ Good up to critical point

$$i' = 1996.7\ T - \left[0.075(n+1)\left(\frac{273}{T}\right)^n - v'\right]p + 1.9441\times10^6\ \text{J/kgK} \qquad \text{(II-9)}$$

or

$i'' = i' + r_c$, which is more accurate than Eq.(7) for saturated steam

$$r_c = 346.6\sqrt[3]{T_k - T}\ \text{[kJ/kg]}\ \text{Latent heat of evaporation} \qquad \text{(II-10)}$$

$$s' = 10.1796\ \log\left(\frac{T}{273}\right) - 8.6229\times10^{-4}(T-273) + 1.8836\times10^{-6}(T-273)^2\ \text{kJ/kg}^\circ\text{K} \qquad \text{(II-11)}$$

$$q = 4.186(t + 2.0\times10^{-5}t^2 + 3.0\times10^{-7}t^3)\ \text{[kJ/kg]} \qquad \text{(II-12)}$$

$$i' = 1 + v'p = q + p\times10^{-6}\ \text{[kJ/kg]}\ \text{Enthalpy of Liquid} \qquad \text{(II-13)}$$

$$v'' = \frac{RT}{p} - 0.075\left(\frac{273.2}{T}\right)^{10/3} + v' = v_a \qquad \text{(II-1)}$$

Eq. (II-8)	By Smith, Keyes & Gerry, 1934 (Plank, R., p. 112)
(II-10)	By M. Jakob, 1935 (Plank, p. 125)
(II-12)	Regnault Data for Spec. Heat of Liquid, see Eq. (II-6)
(II-11)	By integration from (II-12)
(II-13)	By integration from (II-12)
(II-1)	Callendar Eq. of State
(II-9)	From General Eq. of Thermodynamics and Eq. (II-1).

SECURITY CLASSIFICATION OF THIS PAGE (When Data Entered)

REPORT DOCUMENTATION PAGE		READ INSTRUCTIONS BEFORE COMPLETING FORM
1. REPORT NUMBER FINAL REPORT	2. GOVT ACCESSION NO.	3. RECIPIENT'S CATALOG NUMBER
4. TITLE (and Subtitle) 6 Analysis of Two-Phase Flow in Nozzles and Turbine Buckets,		5. TYPE OF REPORT & PERIOD COVERED 9 Final Report, 1 July 1978 - 30 APRIL 1979,
		6. PERFORMING ORG. REPORT NUMBER
7. AUTHOR(s) 10 Emil/Ritzi		8. CONTRACT OR GRANT NUMBER(s) 15 N00014-78-C-0649
9. PERFORMING ORGANIZATION NAME AND ADDRESS Office of Naval Research Department of the Navy 800 N. Quincy Street Arlington, VA 02217		10. PROGRAM ELEMENT, PROJECT, TASK AREA & WORK UNIT NUMBERS 122403 NR 097-422
11. CONTROLLING OFFICE NAME AND ADDRESS DCASMA-LA 9920 S. La Cienega Blvd. Inglewood, CA 90301 11 1 Jun 79		12. REPORT DATE June 1, 1979
		13. NUMBER OF PAGES
14. MONITORING AGENCY NAME & ADDRESS (if different from Controlling Office)		15. SECURITY CLASS. (of this report) Unclassified
		15a. DECLASSIFICATION DOWNGRADING SCHEDULE

16. DISTRIBUTION STATEMENT (of this Report)

See Distribution List

This document has been approved for public release and sale; its distribution is unlimited.

17. DISTRIBUTION STATEMENT (of the abstract entered in Block 20, if different from Report)

12 104 p.

18. SUPPLEMENTARY NOTES

14 108-F

19. KEY WORDS (Continue on reverse side if necessary and identify by block number)

Two-Phase Flow
Nozzle Efficiency
Bucket Flow

20. ABSTRACT (Continue on reverse side if necessary and identify by block number)

A one-dimensional analytical study was made of the two-phase flow of wet steam in a convergent-divergent nozzle with negligible wall friction. The liquid phase is assumed to consist of a cloud of spherical droplets, whose size is either controlled by a critical Weber number or predetermined. Nozzle geometry, phase velocities, mass flux density and local efficiencies are determined by numerical integration from the basic differential equation.
The two-dimensional two-phase flow in impulse turbine buckets was also investigated. The parameters that control the deviation angle of the droplets from the [illegible] ified.

DD FORM 1 JAN 73 1473 EDITION OF 1 NOV 65 IS [illegible]

SECURITY CLASSIFICATION OF THIS PAGE (When Data Entered)

DISTRIBUTION LIST

	No. Of Copies
M. KEITH ELLINGSWORTH Scientific Officer, Director Power Programs Material Sciences Division Office of Naval Research 800 North Quincy St. Arlington, VA 22217	1
RON SULLIVAN Administrative Contracting Officer Defense Contract Administration Services Management Area, Los Angeles 9920 South La Cienega Blvd. Inglewood, CA 90301	1
DIRECTOR, NAVAL RESEARCH LABORATORY Attn: Code 2627 4555 Overlook Avenue Washington, D.C. 20375	6
DEFENSE DOCUMENTATION CENTER Bldg. 5, Cameron Station Alexandria, VA 22314	12
OFFICE OF NAVAL RESEARCH BRANCH OFFICE 1030 East Green Street Pasadena, CA 91106	1